Structure of the SE Greenland margin from seismic reflection and refraction data: Implications for nascent spreading center subsidence and asymmetric crustal accretion during North Atlantic opening

John R. Hopper,[1] Trine Dahl-Jensen,[2] W. Steven Holbrook,[3] Hans Christian Larsen,[1] Dan Lizarralde,[4] Jun Korenaga,[5,6] Graham M. Kent,[7] and Peter B. Kelemen[8]

Received 28 May 2002; revised 3 October 2002; accepted 25 October 2002; published 24 May 2003.

[1] Seismic reflection and refraction data from the SE Greenland margin provide a detailed view of a volcanic rifted margin from Archean continental crust to near-to-average oceanic crust over a spatial scale of 400 km. The SIGMA III transect, located ~600 km south of the Greenland-Iceland Ridge and the presumed track of the Iceland hot spot, shows that the continent-ocean transition is abrupt and only a small amount of crustal thinning occurred prior to final breakup. Initially, 18.3 km thick crust accreted to the margin and the productivity decreased through time until a steady state ridge system was established that produced 8–10 km thick crust. Changes in the morphology of the basaltic extrusives provide evidence for vertical motions of the ridge system, which was close to sea level for at least 1 m.y. of subaerial spreading despite a reduction in productivity from 17 to 13.5 km thick crust over this time interval. This could be explained if a small component of active upwelling associated with thermal buoyancy from a modest thermal anomaly provided dynamic support to the rift system. The thermal anomaly must be exhaustible, consistent with recent suggestions that plume material was emplaced into a preexisting lithospheric thin spot as a thin sheet. Exhaustion of the thin sheet led to rapid subsidence of the spreading system and a change from subaerial, to shallow marine, and finally to deep marine extrusion in ~2 m.y. is shown by the morphological changes. In addition, comparison to the conjugate Hatton Bank shows a clear asymmetry in the early accretion history of North Atlantic oceanic crust. Nearly double the volume of material was emplaced on the Greenland margin compared to Hatton Bank and may indicate east directed ridge migration during initial opening. *INDEX TERMS:* 3025 Marine Geology and Geophysics: Marine seismics (0935); 8105 Tectonophysics: Continental margins and sedimentary basins; 8120 Tectonophysics: Dynamics of lithosphere and mantle—general; *KEYWORDS:* Greenland margin, volcanic rifted margin, mantle dynamics, continental breakup, asymmetric spreading

Citation: Hopper, J. R., T. Dahl-Jensen, W. S. Holbrook, H. C. Larsen, D. Lizarralde, J. Korenaga, G. M. Kent, and P. B. Kelemen, Structure of the SE Greenland margin from seismic reflection and refraction data: Implications for nascent spreading center subsidence and asymmetric crustal accretion during North Atlantic opening, *J. Geophys. Res.*, *108*(B5), 2269, doi:10.1029/2002JB001996, 2003.

1. Introduction

[2] A natural consequence of continental lithospheric extension and breakup is that mantle upwells, decompresses, and melts, leading to the creation of new crust through surface volcanism and subsurface intrusions. The opening of the North Atlantic basin during the Paleocene lead to the creation of an enormous volcanic province, commonly referred to as the North Atlantic Igneous Province (NAIP, Figures 1 and 2). The remnants of the NAIP can be found on the west and east coasts of Greenland, the Faeroe Islands, and the British Isles as thick piles of flood basalts. Offshore, the rifted margins of the North Atlantic show seaward dipping reflector sequences that drilling has demonstrated to be subaerially erupted basalts [*Eldholm et al.*, 1989; *Saunders et al.*, 1998]. These dipping reflectors have become diagnostic features of volcanic margins and

[1]Danish Lithosphere Center, Copenhagen, Denmark.
[2]Geological Survey of Denmark and Greenland, Copenhagen, Denmark.
[3]Department of Geology and Geophysics, University of Wyoming, Laramie, Wyoming, USA.
[4]School of Earth and Atmospheric Sciences, Georgia Institute of Technology, Atlanta, Georgia, USA.
[5]Department of Earth and Planetary Science, University of California, Berkeley, Berkeley, California, USA.
[6]Now at Department of Geology and Geophysics, Yale University, New Haven, Connecticut, USA.
[7]Scripps Institution of Oceanography, University of California, San Diego, La Jolla, California, USA.
[8]Department of Geology and Geophysics, Woods Hole Oceanographic Institution, Woods Hole, Massachusetts, USA.

0148-0227/03/2002JB001996$09.00

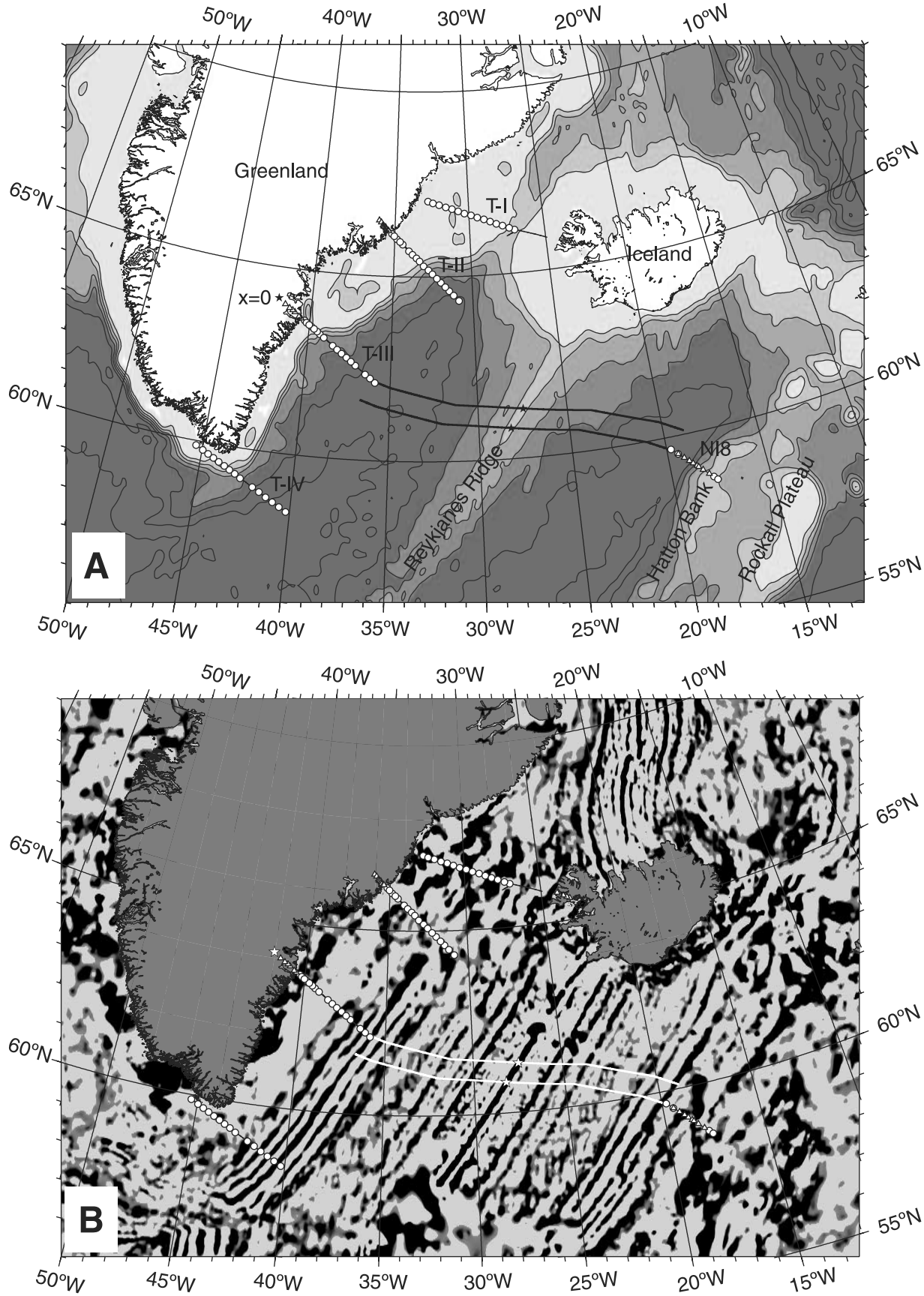
50°W
40°W
30°W
20°W
10°W
65°N
60°N
55°N
45°W
35°W
25°W
15°W
Greenland
Iceland
T-I
T-II
T-III
T-IV
x=0
NI8
Reykjanes Ridge
Hatton Bank
Rockall Plateau
A
B

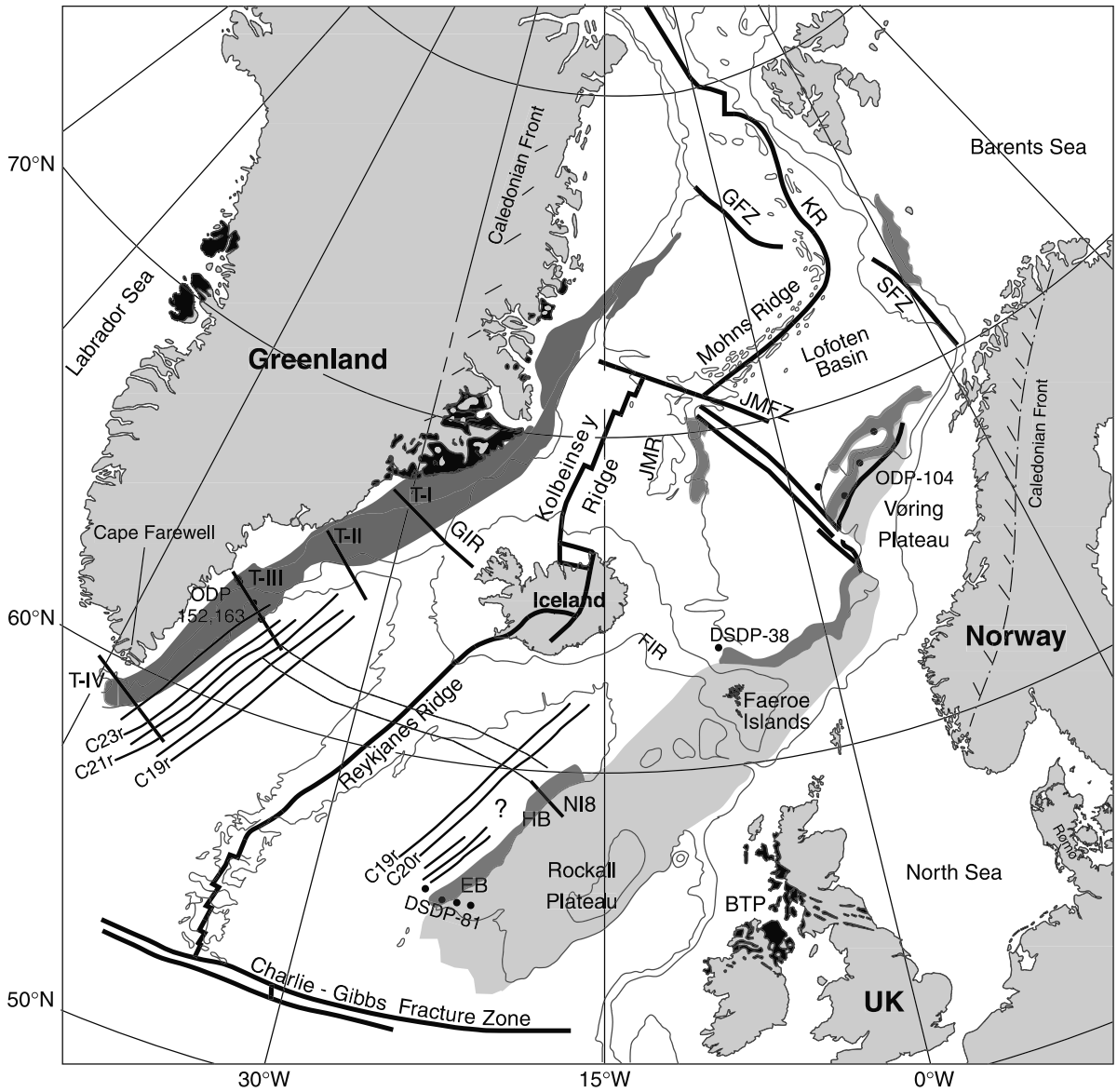

Figure 2. Tectonic and geologic overview of the North Atlantic region. T-1 to T-IV along the East Greenland coast are the SIGMA transects. Thick black lines labeled CXXr are magnetic anomalies. Black areas show where basalts are exposed onshore. Offshore light gray shading shows areal extent of basalt flows and sills associated with initial opening. Offshore dark gray shading shows location of seaward dipping reflectors and by inference thick igneous crust associated with subaerial seafloor spreading. We note that large areal extent should not be confused with large volume. Dots are ODP/DSDP drill sites. Abbreviations are BTP, British Tertiary Province; EB, Edoras Bank; HB, Hatton Bank; GIR, Greenland-Iceland Ridge; FIR, Faeroes-Iceland Ridge.

span thousands of kilometers of margin length from the very southern tip of East Greenland and the conjugate Edoras Bank [*Nielsen et al.*, 2002; *Barton and White*, 1997], to the NE Greenland coast and the conjugate Vøring margin off Norway [*Hinz et al.*, 1987; *Mutter and Zehnder*, 1988; *Eldholm and Grüe*, 1994; *Skogseid et al.*, 1992]. The proximity of the NAIP to the Iceland hot spot strongly suggests that the two are related, but details regarding the

Figure 1. (opposite) Regional setting of SIGMA survey. SIGMA transects T-I to T-IV are shown. Circles represent OBS/H locations and triangles are land stations. All distances on subsequent figures are great circle distances to the reference point marked by the star labeled $X = 0$. The Hatton Bank profile, NI8, reported by *Spence et al.* [1989], *Fowler et al.* [1989], and *Morgan et al.* [1989] is also shown. Circles are OBS stations, and triangles are center points of ESPs. The lines connecting the ends of T-III and NI8 to the Reykjanes Ridge are flow lines based on poles of rotation of *Srivastava and Tapscott* [1986]. The two lines are ~75 km apart. (a) Bathymetry map at 1000 m contour interval. (b) Magnetic anomaly based on *Verhoef et al.* [1992] compilation. Black is normal polarity magnetization.

volumes of material involved, the magnitude and lateral extent of a thermal anomaly, and the rates and mechanisms of emplacement have been lacking.

[3] In this contribution, we report on key data from the SIGMA (Seismic Investigations of the Greenland Margin) experiment that provide important constraints on some of these details. Both normal-incidence reflection and wide-angle refraction data were acquired along four major transects from the southern tip of Greenland up to the Greenland-Iceland Ridge (Figures 1 and 2). We show data from SIGMA III, which is located ~600 km south of the postulated hot spot track. SIGMA III lies in the distal zone defined by *Holbrook et al.* [2001] where volcanic margin formation was transient and the thermal anomaly was modest. The normal-incidence data show distinct changes in the reflective character of the extrusives that we interpret to be related to the emplacement environment, which changes from subaerial to shallow marine, and finally to deep marine as the ridge system evolves. This subsidence can be explained if excess magmatic productivity during breakup results from active upwelling and an associated thermal anomaly in the mantle that may provide dynamic support to the ridge system. Upon exhaustion of the thermal anomaly, the loss of dynamic support and thermal buoyancy led to rapid subsidence of the active ridge axis. We compare the data to the conjugate Hatton Bank and show that volcanic margin formation at this location shows extreme asymmetry, with nearly double the volume of material being emplaced on the Greenland side. We show that the asymmetry must be caused by a very small scale migration of the ridge axis to the east rather than full ridge jumps. The mechanism responsible for this kind of ridge migration requires further investigation.

2. Tectonic Setting

[4] Northward propagation of rifting and seafloor spreading in the Atlantic opened the Labrador Sea by the Late Cretaceous to Early Tertiary, separating Greenland from North America no later than 62 Ma [*Chalmers and Laursen*, 1995; *Srivastava and Roest*, 1999]. A second rift branch propagated northeast at 56 Ma and opened the North Atlantic basins. Greenland was effectively an independent plate from this time until the cessation of spreading in the Labrador Sea at 42 Ma, after which it again became part of the North American plate [*Srivastava and Tapscott*, 1986]. Opening of the North Atlantic was accompanied by huge volcanic productivity, with up to 10^7 km^3 of new crust created in only 3 m.y. [*White and McKenzie*, 1989; *Larsen and Saunders*, 1998]. Deep Sea Drilling Project (DSDP) legs 38 and 81 and Ocean Drilling Program (ODP) legs 104, 152 and 163 sampled volcanic rocks associated with the offshore parts of the NAIP [*Talwani et al.*, 1976; *Roberts et al.*, 1984; *Eldholm et al.*, 1989; *Saunders et al.*, 1998; *H. C. Larsen et al.*, 1999]. The timing of events during North Atlantic opening is exceptionally well constrained by high-precision ^{40}Ar-^{39}Ar geochronology studies together with unambiguous magnetic spreading anomalies south of Iceland from C24r onward [*Sinton and Duncan*, 1998; *Storey et al.*, 1998; *Macnab et al.*, 1992; *Verhoef et al.*, 1992].

[5] A widespread but low-volume volcanic event at 61 Ma has been interpreted to mark the arrival a mantle plume beneath central Greenland. This volcanic activity has been documented in West Greenland [*Storey et al.*, 1998], East Greenland at the base of the main flood basalts [*Sinton and Duncan*, 1998], in the British Tertiary province [*Pearson et al.*, 1996] and on the Faeroe Islands [*L. M. Larsen et al.*, 1999]. The event is also recorded offshore East Greenland along the SIGMA III transect at ODP site 917, where an unconformity separates prebreakup continental sediments from the overlying volcanic pile. The lower and middle series of these rocks consist of 500–800 m of picrites and basalts that give way upward to more evolved basalts and dacites [*Larsen and Saunders*, 1998]. The ^{40}Ar-^{39}Ar age determinations show that they are 60–62 Ma [*Sinton and Duncan*, 1998].

[6] The large volume of the NAIP, however, is primarily expressed in the margins along Greenland, Norway, and the Rockall Plateau, where thick igneous crust was accreted. This thick crust is typified by seaward dipping reflectors that DSDP and ODP drilling off both Norway and Greenland confirmed are subaerially emplaced extrusive basalts that erupted from an Icelandic type spreading center [*Eldholm et al.*, 1989; *Saunders et al.*, 1998]. Along SIGMA Transect III, they are picrites followed by a uniform sequence of depleted Icelandic tholeiites [*Saunders et al.*, 1998]. Geochemical evidence for continental contamination is found only near the base [*Saunders et al.*, 1998], showing that most of the crust associated with the dipping reflector wedge is new igneous crust formed at a spreading center. The flows at the base of the upper series at ODP site 917 unconformably overly the 60–62 Ma lower and middle series rocks. They have been dated to 55.8 Ma and flows at ODP site 918 from the central part of the dipping reflector wedge have been dated to 54.0 Ma [*Tegner and Duncan*, 1999]. The youngest part has not been sampled, but the dipping reflectors end within magnetic anomaly C24n at ~53 Ma, indicating that the entire sequence was emplaced in less than 3 m.y.

[7] On the basis of the full SIGMA data set (Figure 1), *Holbrook et al.* [2001] define two zones depending on proximity to the presumed location of the Iceland hot spot. The proximal zone is localized to within 300 km of the Iceland hot spot and shows crustal thicknesses on the order of 30 km. Both the Greenland-Iceland Ridge and the Faeroe-Iceland Ridge have crust this thick [*Smallwood et al.*, 1999; *Holbrook et al.*, 2001] and are thought to mark the track of a plume stem that has been more or less centered near the Mid-Atlantic Ridge for most of the last 50 m.y. Present-day Iceland itself has highly variable thicknesses, but is on average 29 km thick [*Allen et al.*, 2002]. Along the Greenland Iceland Ridge where the seismic velocity structure is best constrained, the average V_p is less than would be predicted by passive upwelling models, supporting the idea that this crust is created over a region of robust active upwelling that a plume stem might produce [*Kelemen and Holbrook*, 1995; *Holbrook et al.*, 2001; *Korenaga et al.*, 2002]. Material flux through the solidus of 3 to 4 times greater than plate driven upwelling are needed over the plume stem [*Holbrook et al.*, 2001]. The distal zone shows both reduced crustal thickness and reduced average seismic velocity. *Holbrook et al.* [2001] suggest that little to no active upwelling is required in the distal zone and that excess crustal thickness is primarily a result of passive rifting over a modest thermal anomaly on the order of

100°C, which may be consistent with the geochemical data [*Tegner et al.*, 1998]. This latter conclusion is highly dependent on the assumed source composition and a smaller thermal anomaly would be consistent with melting of a more Fe-rich mantle source [*Korenaga and Kelemen*, 2000; *Korenaga et al.*, 2002].

[8] A result of the data summarized above is that the original plume hypothesis for the formation of the NAIP has undergone significant revision. To explain the large lateral extent of volcanic margin formation in the context of passive rifting models, it was suggested that newly rising mantle plumes generate huge heads that balloon beneath the lithosphere [*White and McKenzie*, 1989; *Griffiths and Campbell*, 1990; *Hill*, 1991]. Subsequent rifting over the hot plume head was thought to be responsible for volcanic margin formation while sustained excess volcanism only occurred over a restricted region defined by the plume stem, marked by the Greenland-Iceland-Faeroes ridge. Large plume heads ballooning beneath the lithosphere, however, have proven problematic and are inconsistent with several lines of evidence as summarized by *Nielsen et al.* [2002] and *Larsen and Saunders* [1998]. They suggest an alternative in which a rising plume with only a modest or no head impacts the base of the lithosphere and spreads rapidly into a thin sheet of material that fills lithospheric thin spots and is blocked by thick spots [*Nielsen et al.*, 2002]. This simple modification to the plume model is consistent with the geochronology and geophysical data summarized above, and we show is consistent with the data along the SIGMA III transect presented below.

3. Data Acquisition and Processing

[9] Data were acquired in 1996 on the R/V *Maurice Ewing* using a 20-air gun 138 l (8460 cu. in.) tuned source array. For reflection imaging, the data were recorded on *Ewing*'s 4-km 160-channel digital streamer, which had a receiver group spacing of 25 m. Wide-angle data were recorded on eleven WHOI OBHs, eight U.S. Geological Survey OBSs, and six onshore portable seismometers from the Program for the Array Seismic Studies of the Continental Lithosphere (PASSCAL). The total length of the profile is nearly 400 km, and all horizontal distances are measured from a common reference point (Figure 1).

3.1. MCS Data

[10] Guns were fired at a 21 ± 1 s interval for a nominal shot spacing of ~50 m. The actual shot spacing varied from 30 to 62 meters with an average spacing of 51.56 m. Data were recorded at a sampling interval of 2 ms and resampled to 4 ms prior to processing. Data were binned into common midpoint gathers spaced every 12.5 m along the profile. This yields a nominal fold of 40 with a 50 m shot point spacing and 160 channels. To process the data, we first applied a spherical divergence correction using stacking velocity functions from previous data collected in the region. The near channels show significant 8 Hz noise that we suppressed by including a narrow, 0.25 Hz wide notch filter on the inner 1.2 km of the streamer. The data were then band-pass filtered from 3 to 60 Hz.

[11] Stacking velocities were picked from semblance analyses computed at control points determined by lateral structural changes seen in the data (Figure 3). Semblance was computed by combining 4 CMPs at each control point to create supergathers that have traces at every receiver offset location. The velocities picked were then used to construct average velocity functions for the deep water section (>2 s two-way travel time (twt)) and the shallow water section (<1 s twt). These average functions were used for calculating common offset *f-k* dip moveout (DMO) on the data. Lateral velocity variations clearly exist in the data, but the DMO processing seemed robust nonetheless and improved the image quality. After DMO, semblance was rerun and the velocities repicked.

[12] Multiple energy proved the most difficult challenge on this data set. We attempted a variety of demultiple techniques, none of which was completely adequate. After some experimentation, we finally arrived at a three-step process that included *f-k* space velocity filtering, a severe inner trace mute, and median stacking.

[13] The *f-k* velocity filtering was done on supergathers created by combining every four CMPs. To maintain the even spatial sampling required by the Fourier transforms, missing offsets in the supergathers were filled with interpolated traces prior to transformation. The filtering was achieved by applying a moveout correction at 85% of the picked stacking velocities, transforming the data to *f-k,* and then discarding the positive wave numbers before transforming back to *t-x* [e.g., *Yilmaz*, 1987]. Because the filter is applied in a way that energy near the 0 wave number axis is not affected, multiples in the near traces of a CMP gather are not attenuated. Therefore we also applied an inner trace mute beginning at twice the water bottom time on the 45 channels nearest to the ship. The final stack was produced by using a median stack, which we found further suppressed multiple energy without affecting the primaries [see also *Korenaga et al.*, 2000]. Nevertheless, residual multiple energy is apparent throughout the section and limited our ability to fully migrate the section since significant overmigration noise degraded the stack and made the section difficult to interpret. We instead applied a poststack migration at water velocity, which combined with the prestack DMO means that the data are only partially migrated. The final time section is shown in Figure 3. The overall data quality is very good and the shallow structures are especially well imaged. Deep reflections are conspicuously absent despite the fact that previous surveys show indications of lower crustal reflectivity [*Larsen et al.*, 1998]. A series of constant velocity stacks were constructed to attempt to determine if deeper structure such as reflection Moho could be imaged in the data, but this proved unfruitful.

3.2. Wide-Angle Data

[14] The wide-angle data are generally high quality. The OBH/S record sections were recorded simultaneously with the MCS acquisition and thus have a 50 m shot point interval. Poor weather conditions onshore prevented the complete deployment of the REFTEK stations and we reshot part of the line after the MCS work to ensure that we had data on land. For the reshoot, guns were fired every 50 ± 1 s for a nominal shot spacing of 125 m. Wide-angle stations were deployed along the same great circle arc that the MCS data were collected along. This arc passes through 42°02′38.4″N, 64°09′40.0″W (reference point in Figures 1

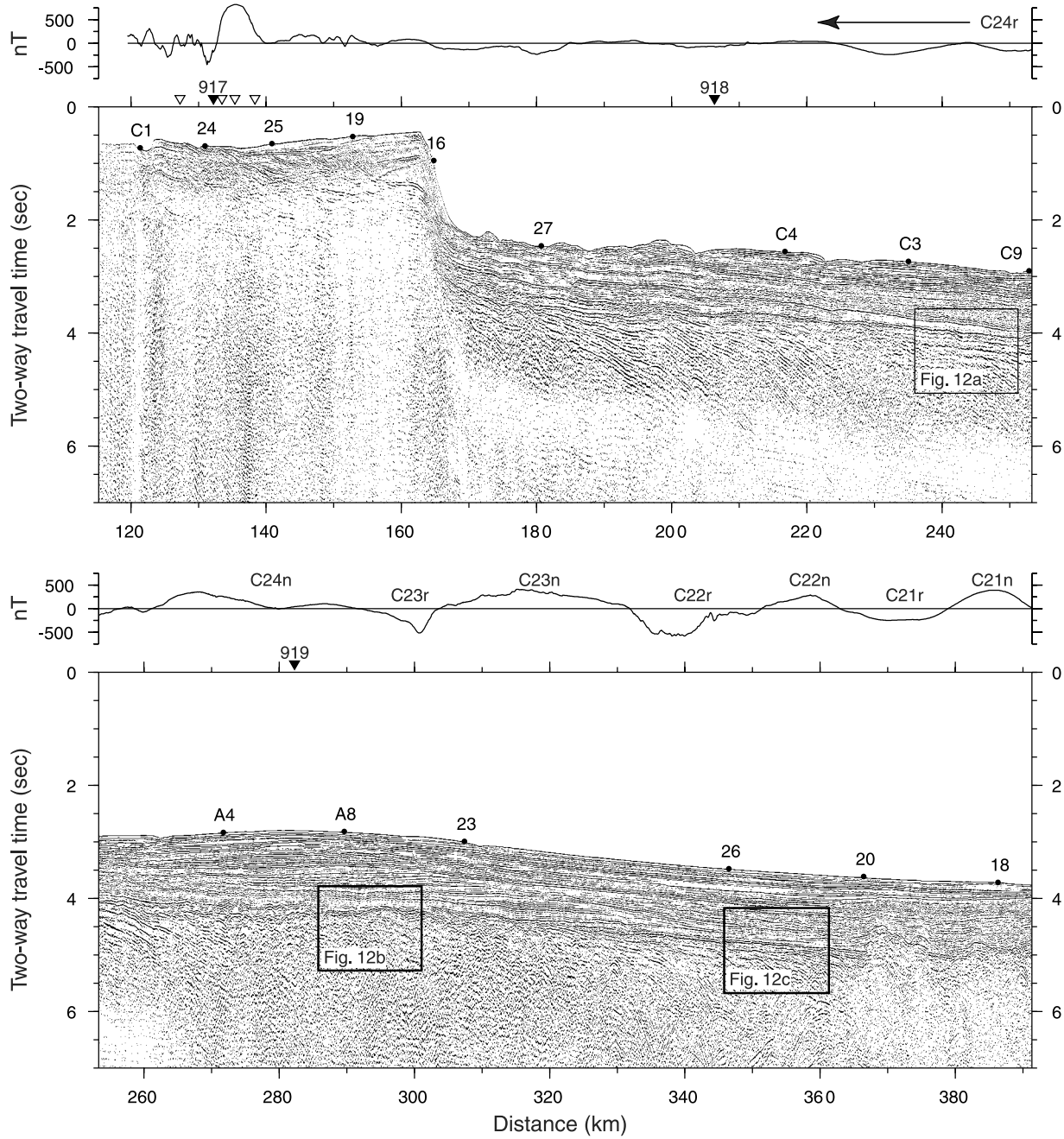

Figure 3. Uninterpreted MCS data from SIGMA T-III. See text for data processing information. Dots are ocean bottom stations: USGS OBSs are designated with alpha-numeric labels and WHOI OBHs are designated with numeric only labels. Triangles are ODP Leg 152 and Leg 163 drilling sites. Unlabeled open symbols are Sites 989, 916, 990/915, and 914 from left to right. Magnetic anomaly is from the shipboard magnetometer and interpreted spreading anomalies are labeled.

and 2) and 35°48′09.0″N, 64°04′29.5″W and defines the 2-D plane along which velocity modeling was done. After relocation, instrument positions were projected onto the plane. The ocean bottom stations were mostly within a few hundred meters of this plane, with an average off-line distance of 100 m and the largest off-line distance nearly 700 m (OBS C1). Placement of the land stations was limited by finding suitable locations along the fjord and vary from 400 to 2640 m off line. For both land and ocean bottom stations, instrument clocks were synchronized to GPS time before and after deployment and linear clock drift corrections applied. The maximum correction was 0.4 ms/h, and the average was 0.1 ms/h.

[15] Data were recorded with a sampling interval of 10 ms and were band-pass filtered from 4 to 20 Hz. The main difficulty with the wide-angle data is that previous shot noise often obscures the low amplitude but very coherent arrivals at larger offsets. This was a problem on the data used by *Holbrook et al.* [2001] and we reprocessed the data using a different *f-k* based velocity filter to remove the

previous shot noise. This reprocessing led to significant improvements to the data. After the *f-k* filter, a minimum phase Wiener-Levinson predictive deconvolution was applied. The filters and deconvolutions introduce sidelobe energy and small shifts in the data that need to be taken into account for accurate travel time modeling. The effects of these were checked and adjusted for by comparing the direct arrivals on the OBH/S's to the seafloor arrival on the MCS data and to the hydrosweep center beam depth. The latter two agree to within 10 ms along the entire line and provide a reasonable check on the direct arrivals.

4. Margin Structure and Velocity Model

[16] The new seismic data set provides a clear and detailed view of a volcanic rifted margin from continental crust to near-average oceanic crust as defined by *White et al.* [1992]. In this section, we first discuss the velocity modeling and key aspects of the wide-angle data and then summarize the main features of the reflection data. To distinguish between relative distances and measurements, we refer to absolute position along the profile as km X, where X is the distance from the common reference point shown in Figure 1.

4.1. Velocity Modeling of Wide-Angle Data

[17] To examine in closer detail crustal accretion processes in the distal zone away from the Iceland plume track, we remodeled the wide-angle data presented by *Holbrook et al.* [2001] on the reprocessed data set. The first arrivals that were picked on each instrument were verified, corrected where necessary, supplemented with new picks where appropriate and then checked for reciprocity with neighboring instruments. We then used iterative ray tracing and inversion to determine the velocity structure [*Zelt and Smith*, 1992]. Essentially, we did an automated forward modeling using *Zelt and Smith*'s [1992] inversion as a guide to determine how best to change the model to fit the data. The model was constrained to fit two pieces of a priori information, namely, the seafloor depth and the basement two-way travel time, which are known to high accuracy from bathymetry data and MCS data, respectively. The primary goal of the velocity modeling was to determine the large-scale velocity structure and crustal thickness variation across the margin.

[18] Figure 4 shows large-scale plots of an OBH from on the shelf and an OBS from deep water in the Irminger Basin. Figure 5 shows the remaining instruments at smaller scale. All the stations show clear crustal refraction arrivals ($P_{2\&3}$) and reflections from the Moho (P_mP), which are the most important arrivals for constraining the large-scale crustal structure. The model contains a water layer, two layers within the sediments, and two layers within the basement, which is igneous oceanic crust on the seaward end and continental crust on the landward end. The two layer oceanic crust is necessary because two distinct sets of crustal refraction arrivals are seen that correspond to arrivals from oceanic layers 2 (P_2) and 3 (P_3) (Figure 4). We also include two layers in continental basement because of evidence on the REFTEKs for reflectivity at ~16 km depth (Figure 5). Some of the stations show weak arrivals that are P_n, but because they are very weak and are not seen consistently, we did not attempt to model them and thus have no constraints on the mantle velocity.

[19] The final model is shown in Figure 6 and differs only slightly from the model published in *Holbrook et al.* [2001]. Layer boundaries are defined by 15–20 nodes accept for the seafloor and basement, which are defined by 90 nodes since they are known to high resolution from bathymetry and MCS data sets. Crustal layers are defined by 10–19 velocity nodes and care was taken to include velocity nodes only when necessary to fit particular aspects of the data. In this way we minimize the introduction of unrequired structure. A summary of the ray coverage is shown in Figure 7 showing bottoming points of crustal refractions and reflection points from the Moho. In general the ray coverage is excellent from the continent-ocean boundary (COB) and through the section of anomalously thick oceanic crust. In total, the model is constrained by 2933 P_2, P_3 and P_mP travel time picks and the average RMS misfit between the calculated and observed travel times is 0.122 s with a normalized chi-square value of 1.488 for an assumed average pick uncertainty of 0.1 s. Over oceanic crust, the fit is considerably better and the RMS misfit seaward of km 160 is less than 0.1 s.

[20] From km 0 to km 80 is continental crust, with generally low velocities and gradients that are expected for Archean crust dominated by a felsic composition. The crust is assumed to be ~32–33 km thick, but this is not constrained by the arrivals on the land stations, which indicate a steeply dipping Moho from km 80 to km 150. The deepest bottoming points are from ~31 km depth and a flattening of the Moho at 32–33 km depth is a reasonable assumption for this setting. Estimates of crustal thickness from other Archean terrains in the region vary from ~28 to 38 km [*Chian and Louden*, 1992; *Reid*, 1996; *Funck and Louden*, 1998]. Figure 8 shows a comparison of a velocity profile over continental crust from our model to published profiles from these terrains and the match is quite good. In addition, recent receiver function analyses from broadband seismometers onshore along E. Greenland yield preliminary estimates of ~34 thick Archean crust [*Dahl-Jensen et al.*, 2003].

[21] Between km 150 and km 160 the steeply dipping Moho becomes less steep, and the average crustal velocities and gradients increase. Although it is not possible to use seismic velocity alone to distinguish between continental crust and oceanic crust, we interpret this to mark the COB based on the fact that this is where we can begin to divide the basement into two distinct layers with velocities typical for oceanic layer 2 and 3 [*White et al.*, 1992; *Mutter and Mutter*, 1993]. The location of the velocity change is also fairly well resolved. Moving the boundary 20 km in either direction leads to unacceptably large travel time misfits. In addition, this placement of the COB is in remarkably good agreement with *Larsen and Saunders* [1998] based on ODP drilling and earlier seismic reflection data, giving us confidence that we have located the COB reasonably well. The crust here is 20 km thick, indicating modest continental thinning prior to breakup. However, the lower crustal velocities increase steadily in the region from km 100 to km 150 and could be interpreted as evidence for mafic intrusions and/or underplating that has rethickened the crust. The ocean drilling summarized earlier covers the area from

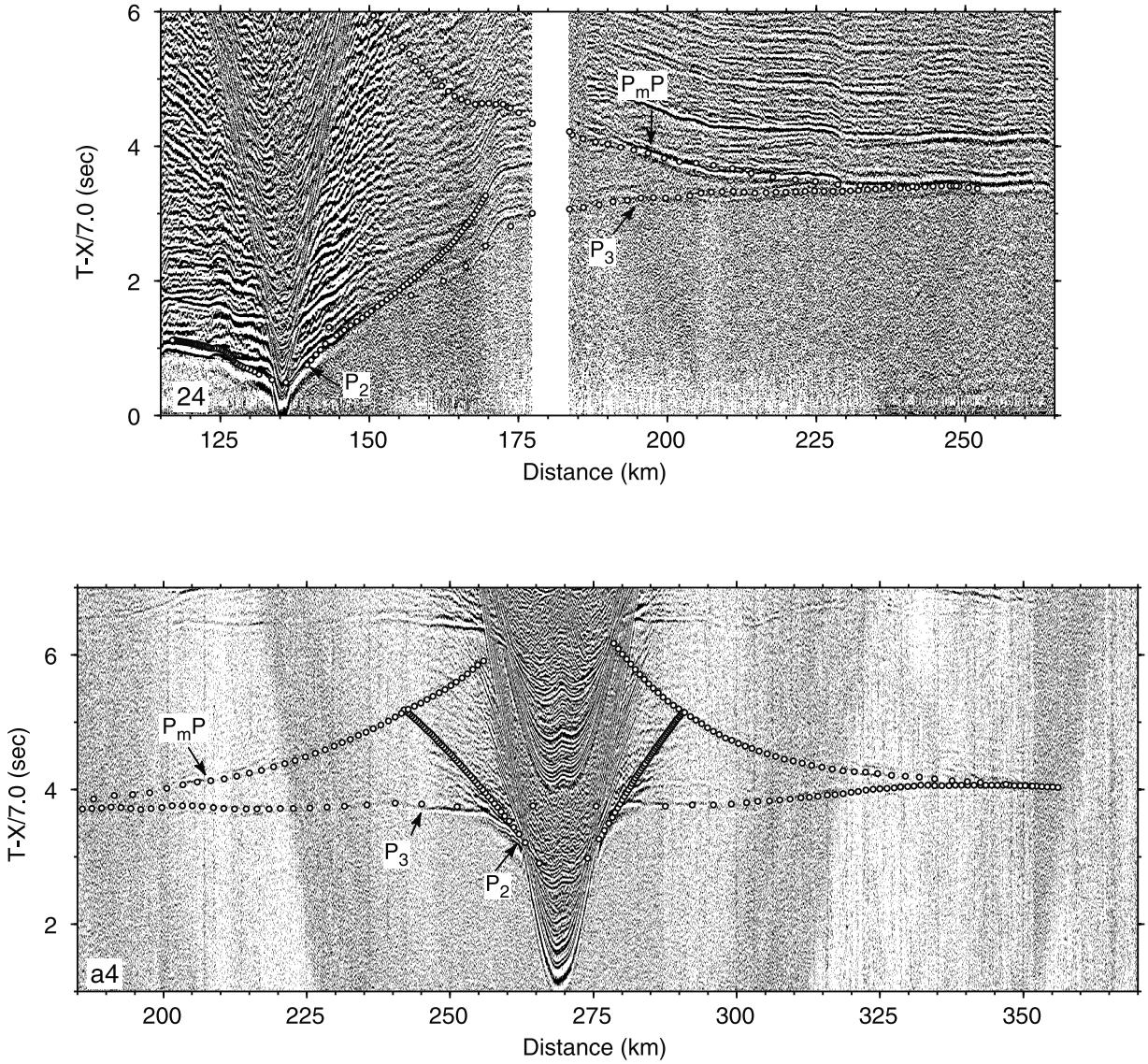

Figure 4. Large-scale plots of representative wide-angle record sections. OBH 24 from on the shelf, and OBS A4 from the deeper ocean basin are shown. White dots are calculated travel time arrivals from 2-D ray tracing based on work by *Zelt and Smith* [1992]. Calculated travel times are for all rays, not just those constrained by travel time picks. Only arrivals from igneous basement are shown.

km 130 to km 140, where the breakup and prebreakup basalt flows are underlain by continental sedimentary basins, supporting the notion of a narrow continent-ocean transition comprised of both attenuated continental crust and new igneous material. Nonetheless, evidence for continental crust that has thinned by more than a factor of two before final breakup is absent and the data support an abrupt COB.

[22] Thus, by km 160–170, the entire crust is new igneous material accreted to the continent. The maximum igneous crustal thickness is 18.3 km and thins gradually over the remaining part of the transect, ending in ~9 km thick oceanic crust (Figures 6 and 9). Despite the relatively constant decrease in crustal thickness, the seismic velocity structure stays fairly uniform from km 160 to km 270–280, at which point the high-velocity lower crust appears to begin to disappear. The maximum velocity in the lower crust is just over 7.5 km/s and the 7.5 km/s contour terminates at km 275. Because no rays turn in the lower crust (Figure 7), accurate determination of the velocity in the deep crust depends primarily on errors in estimating the Moho depth from P_mP reflections. Appropriate caution should therefore be taken with this evidence for reduced lower crustal velocity. Nonetheless, the initial constancy of seismic velocity followed by a decrease is demonstrated more clearly in Figure 9 where average V_p in the crust is plotted as a function of model distance using the same method as *Korenaga et al.* [2000] and *Holbrook et al.* [2001]. Velocities less than 6.85 km/s are assumed to be due to alteration and/or porosity and are replaced by this value prior to averaging. The value 6.85 km/s was chosen because it is the appropriate velocity for the amount of SiO_2 and MgO found in basalts sampled during ODP Leg 152 [from *Kelemen and Holbrook*, 1995, equation (1)]. The velocity is then corrected to a temperature of 400°C and a confining pressure of 600 MPa before averaging (see

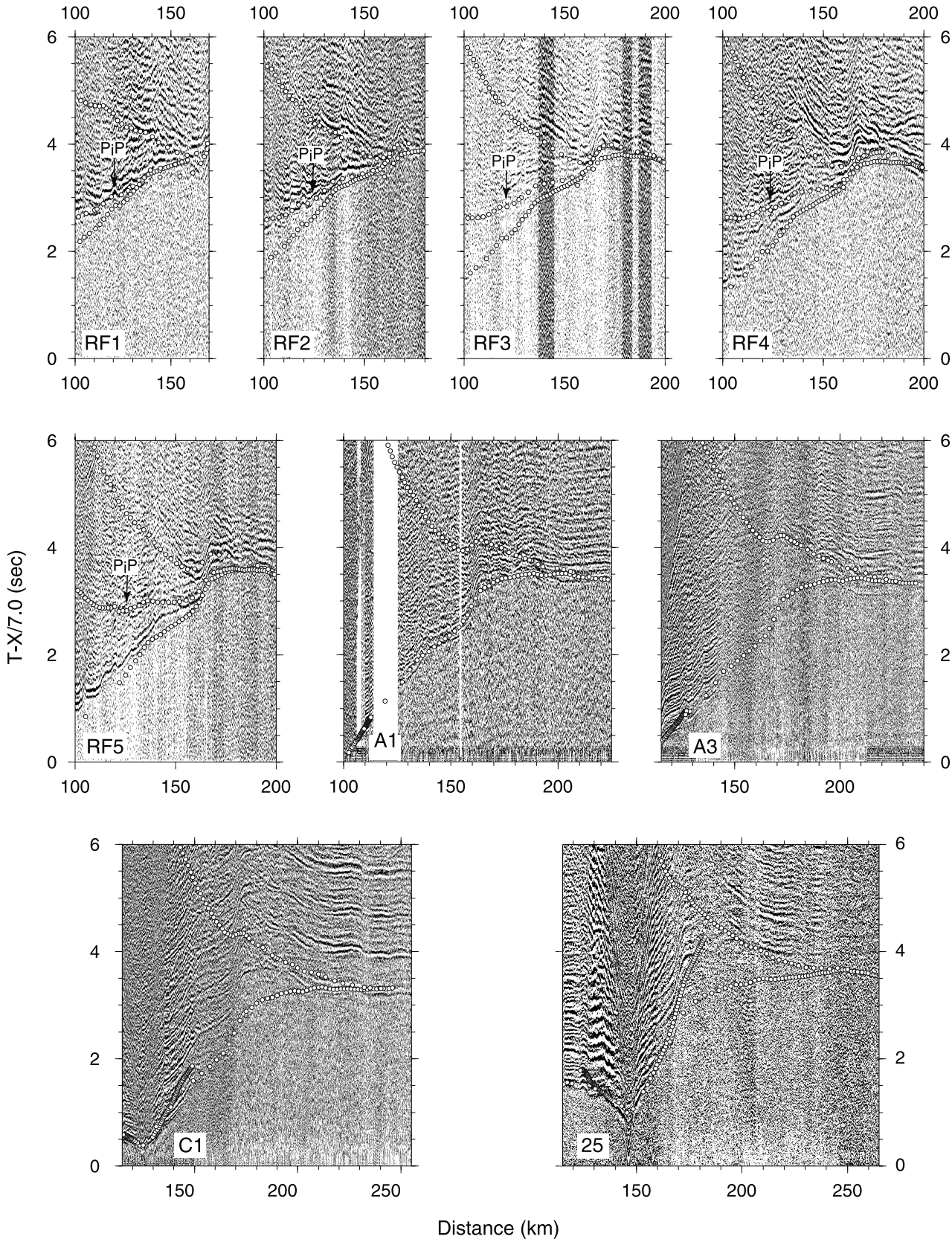

Figure 5. Compilation of all wide-angle record sections used in constraining crustal velocity structure along SIGMA T-III. Plots labeled RFx are the REFTEK land stations and the mid crustal reflection is labeled P_iP on these plots (see text). White dots are calculated travel time arrivals from 2-D ray tracing based on work by *Zelt and Smith* [1992]. Calculated travel times are for all rays, not just those constrained by travel time picks. Only arrivals from igneous basement are shown.

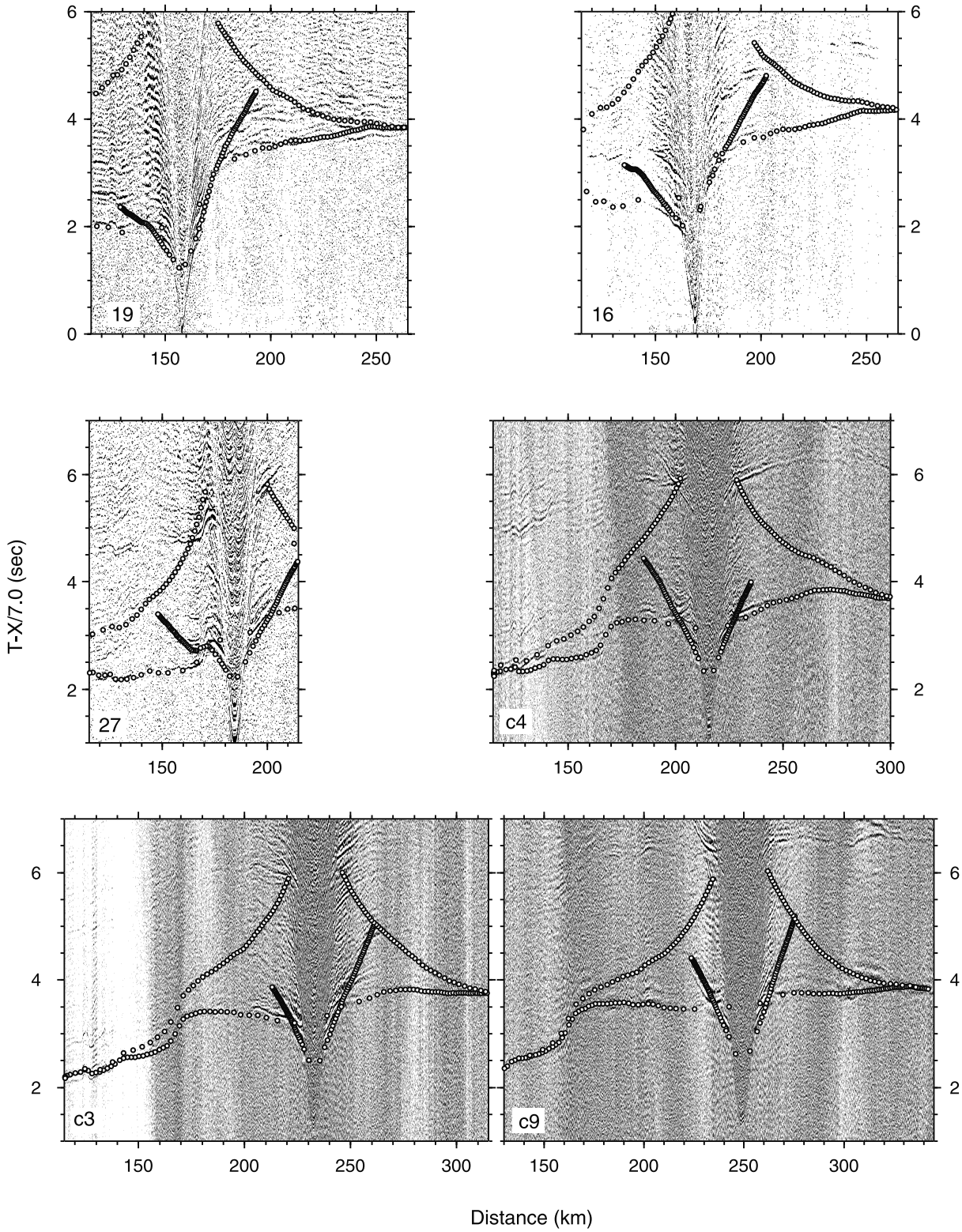

Figure 5. (continued)

Holbrook et al. [2001] and *Korenaga et al.* [2002] for an explanation of this last correction).

[23] *Kelemen and Holbrook* [1995] argued that average V_p and crustal thickness (H_c) combined provide a measure of the bulk crustal composition, which in turn is related to the dynamics of mantle upwelling and melting. Pure passive upwelling will produce thicker crust at higher temperatures by increasing the depth range over which melting occurs. Deeper melts associated with higher temperatures increase the magnesium content and decrease the silicon content of

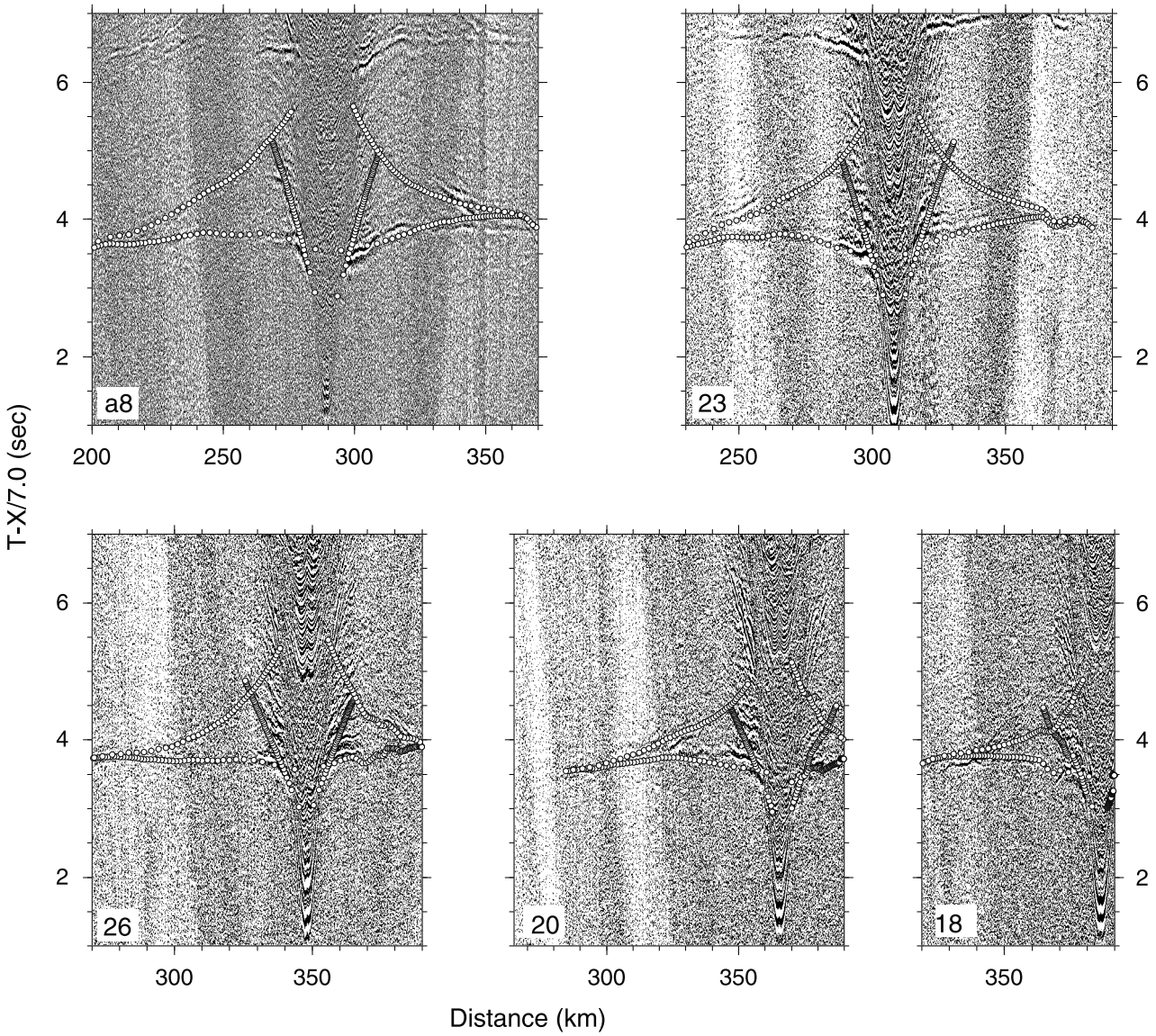

Figure 5. (continued)

the crust and lead to a higher average seismic velocity. In contrast, a component of active upwelling will increase the flux of material through the solidus and generate more melt and thicker crust without substantially altering the depth of melting. In this case, thicker crust can be produced without modifying the average crustal velocity. This approach to using H_c-V_p systematics to estimate crustal composition to constrain the mantle upwelling and melting regime has recently been revised by *Korenaga et al.* [2002], who suggest that the initial study may systematically underpredict seismic velocity for a given crustal composition.

[24] Figure 10 shows the SIGMA III wide-angle data plotted on H_c-V_p diagrams using the equations of *Kelemen and Holbrook* [1995] and those of *Korenaga et al.* [2002]. Two key issues to consider are the uncertainty of the bulk crustal velocity measurement and, assuming that trends are robust given these uncertainties, whether or not a reasonable petrological inference can be made to relate the data to the upwelling dynamics. The change in seismic velocity associated with variations in both mantle potential temperature and the degree of active upwelling is relatively small. Because it is seismic velocity rather than crustal thickness that is most important for the petrological interpretation, this is crucial and these two issues are closely related [*Korenaga et al.*, 2002]. Assessing the velocity versus depth ambiguity inherent in P_mP travel time modeling requires a robust tomographic inversion scheme like that of *Korenaga et al.* [2000]. Although such an inversion was not done here, the results of extensive error analysis in *Korenaga et al.* [2000] suggest that an average velocity error on the order of 1% over the igneous crust where there is dense ray coverage is reasonable for data of this quality. Models that resulted from automated forward modeling on SIGMA II were only slightly different from the inversion results and were within this level of uncertainty [*Korenaga et al.*, 2000; *Holbrook et al.*, 2001]. In addition, we note that trends and slopes resolved by the data were shown to be robust despite large absolute uncertainties. On the basis of these error estimates for data of this quality, we include error bars of ±0.075 km/s for V_p and ±1 km for H_c, but it should be emphasized that

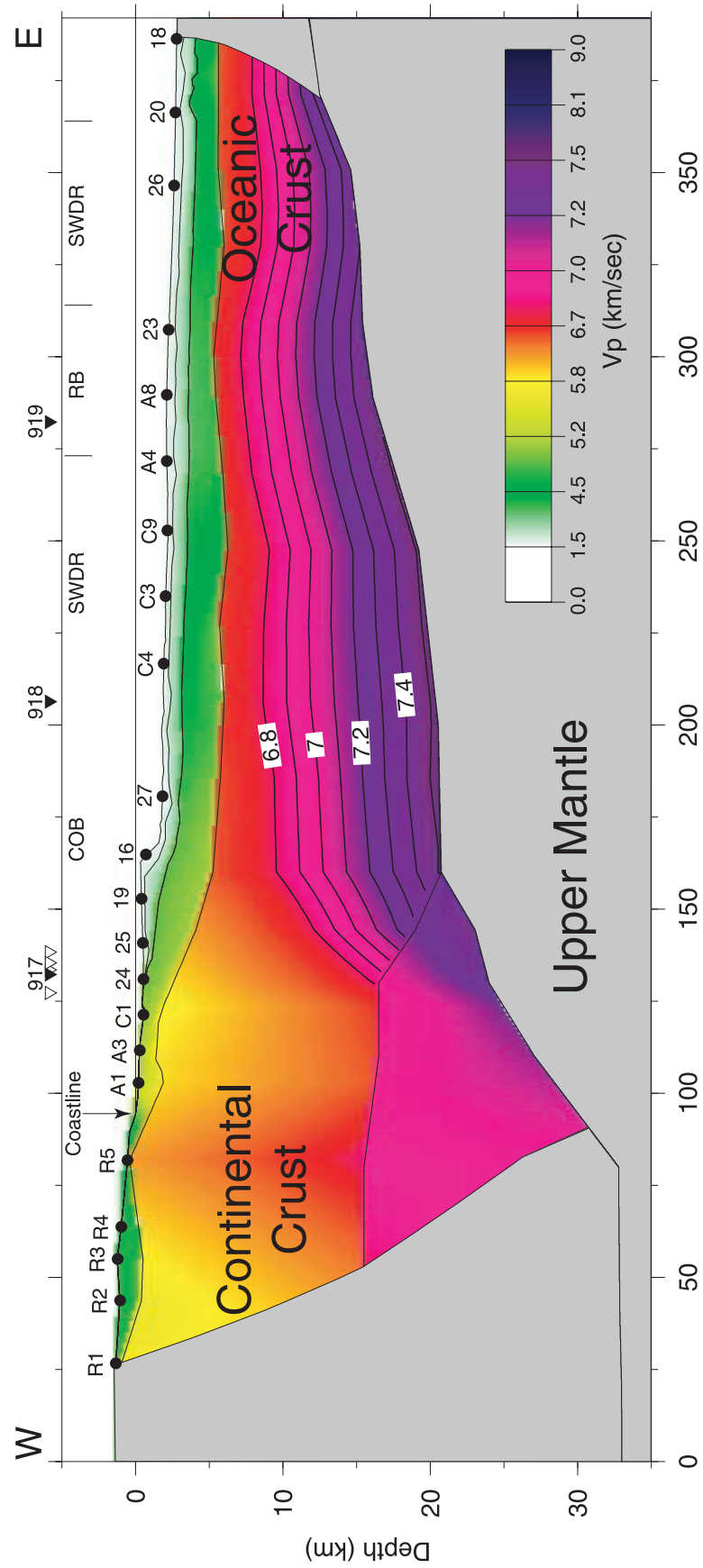

Figure 6. Final velocity model derived from ray tracing along the SIGMA III transect. Velocity contours from 6.8 to 7.4 km/s shown in the oceanic crustal section. Triangles along the top are the ODP drill sites as before. Lower white line is the Moho. Areas not constrained by modeled arrivals are gray. The continent-ocean boundary (COB) as well as the morphological zones based on the reflection data are also marked (Figures 10 and 11; SWDR, seaward dipping reflectors; RB, rough basement).

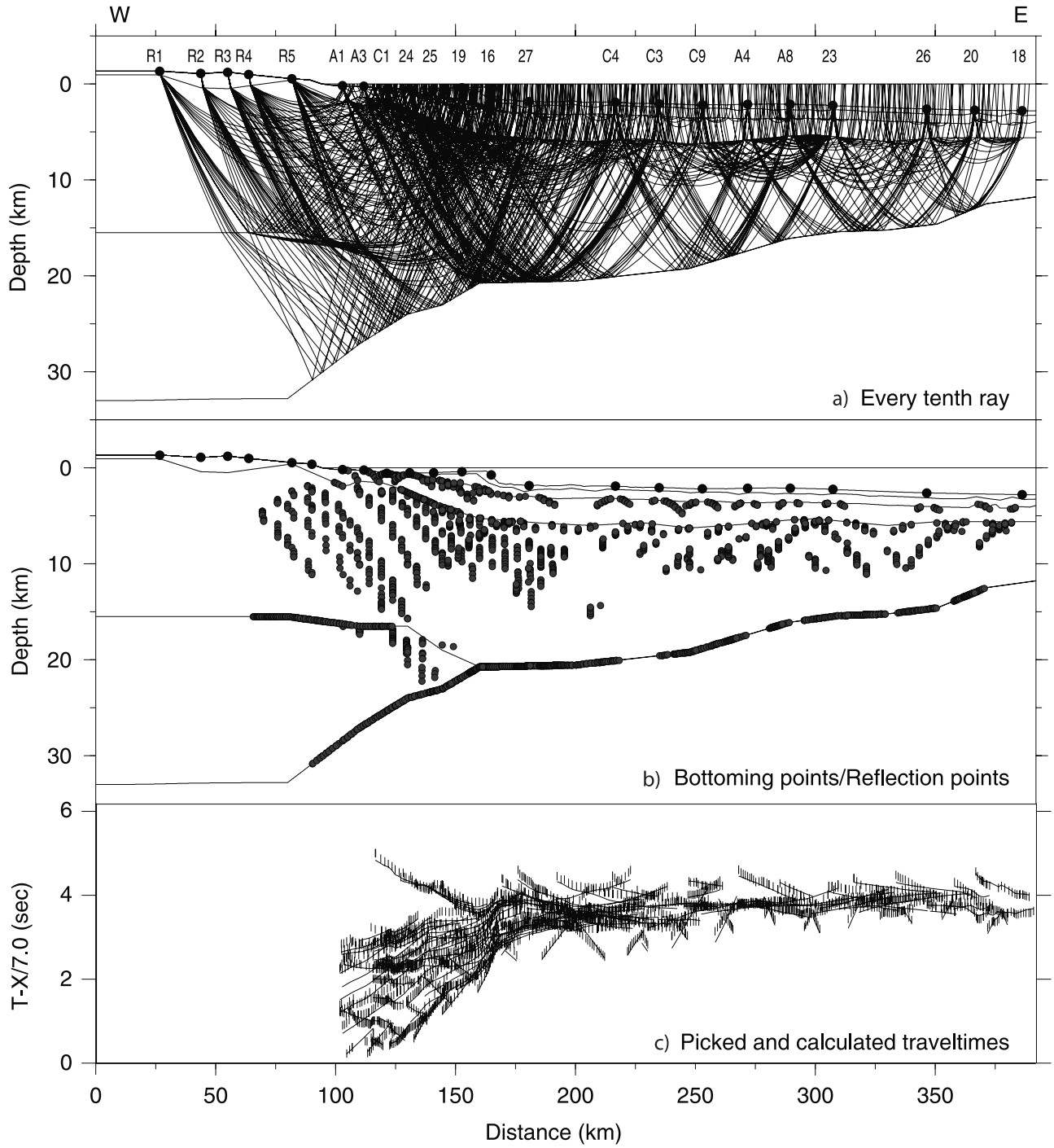

Figure 7. Ray coverage along the transect. Only rays penetrating igneous crust and that are constrained by travel time picks are shown (i.e., point-to-point ray tracing). Every tenth ray is shown. (a) Rays traced for each station. (b) Bottoming points of turning rays and reflection points from the rays shown above in Figure 7a. (c) Picked and calculated travel times for P_2, P_3, and P_mP for all stations. Vertical bars are picked travel times with a bar length of 0.1 s, and lines are ray-traced travel times.

this is not based on a rigorous inversion scheme and error analysis.

[25] The data here show a relatively low bulk velocity despite the very thick crust, and two trends are seen in the data as the margin evolves. The first trend shows a reduction in crustal thickness with no change in average velocity, and a second trend is indicated by an inflection point at ~km 280, beyond which thinner crust is correlated with lower average seismic velocity. The first trend may indicate that margin evolution occurred over a constant potential temperature mantle where the degree of active upwelling decreased with time. In the *Kelemen and Holbrook* [1995] diagram (Figure 10a), the amount of active upwelling is small and there is a modest thermal anomaly present,

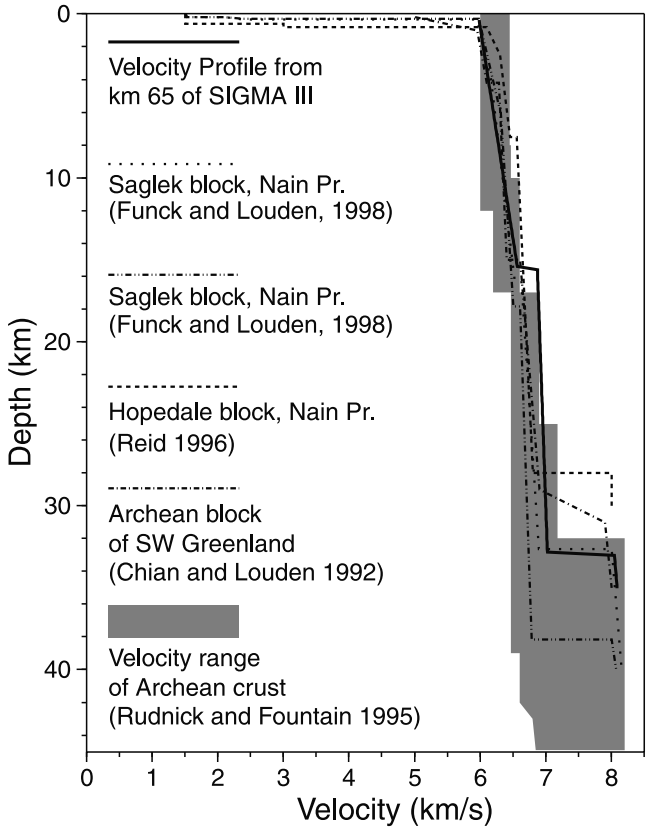

Figure 8. Velocity-depth functions of the SIGMA III data compared to other Archean terrains in the region.

consistent with *Holbrook et al.*'s [2001] suggestion that the distal zone has very little active upwelling compared to the Iceland plume track and that most excess crustal thickness is a result of anomalously warm mantle. The second trend could then be a result of exhaustion of the thermal anomaly that leads to a decrease in both seismic velocity and crustal thickness as a pure plate driven flow is established over normal temperature mantle. Although the absolute potential temperature of the mantle depends on the assumed source composition and melting model, the observed decrease in seismic velocity can be achieved by a reduction in mantle potential temperature of ~100°C [*Kelemen and Holbrook*,

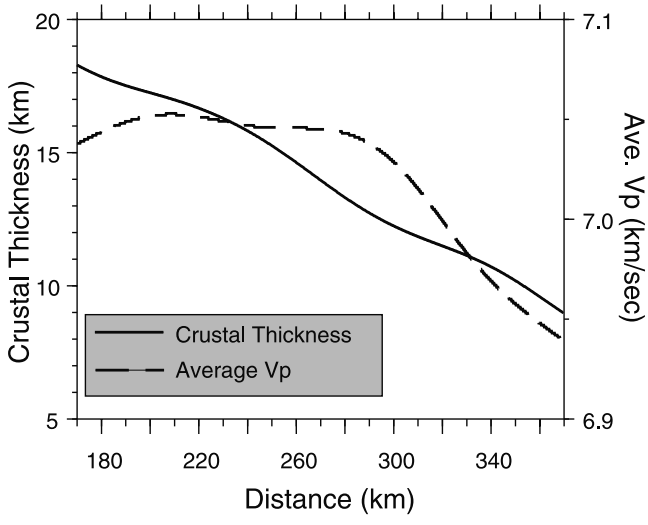

Figure 9. Crustal thickness and average velocity as a function of distance along the transect from km 170 (approximate continent-ocean boundary) to the end of line. Crustal thickness decreases nearly linearly along the profile, while the average seismic velocity is constant for the first half of the profile before decreasing toward more normal oceanic velocities.

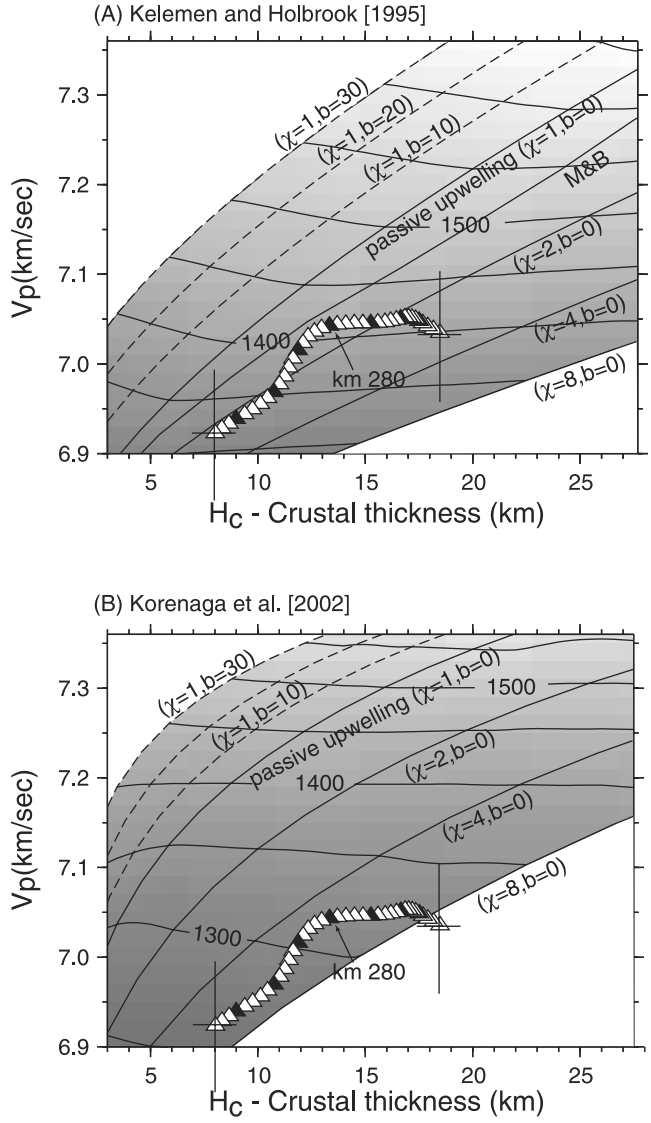

Figure 10. Plots of crustal thickness versus average crustal seismic velocity along the SIGMA III transect. Nearly horizontal lines are potential temperature contours. Sloping lines are different upwelling dynamics where χ is the ratio of mantle upwelling rate to the surface divergence rate and b is the thickness of the lithospheric lid. See *Korenaga et al.* [2002] for details and assumed melting function. The average velocity is for a temperature of 400°C and a pressure of 600 MPa. Curve labeled M&B is for reference to passive upwelling using the melting function of *McKenzie and Bickle* [1988]. See text for explanation of error bars. (a) Systematics based on the relations in *Kelemen and Holbrook* [1995]. (b) Systematics based on the relations of *Korenaga et al.* [2002].

1995; *Korenaga et al.*, 2002]. This scenario is consistent with recent work that suggests mantle plume material was emplaced as a thin sheet of material that filled a thin spot along the proto-North Atlantic basins [*Nielsen et al.*, 2002]. Initial crustal accretion should be associated with constant potential temperature mantle until the thin sheet is exhausted, after which a cooling trend is predicted. We note, however, that this interpretation of the H_c-V_p diagram may not be unique (see discussion by *Korenaga et al.* [2002]). An alternative interpretation is that there is no thermal anomaly present and all excess crustal thickness is a result of active upwelling (Figure 10b). The decrease in crustal seismic velocity could be a function of increased residual crack porosity associated with reduced lithostatic pressure due to thinner crust, an effect that cannot be quantified with existing data [*Korenaga et al.*, 2002] and further work to establish a more robust connection between crustal velocity and mantle dynamics is warranted.

4.2. Reflection Data

[26] The reflection data along SIGMA III show that the transect can be divided into distinct zones based on the reflection characteristics of the upper crust and the lateral coherence of the top basement reflector. A basic interpretation is summarized in Figure 11, and an enlargement of three areas highlighting the differences in reflection characteristics is shown in Figure 12. The landwardmost zone is defined by a coherent reflector defining the basement with top lap of internal seaward dipping reflectors (Figures 11 and 12a). Mafic volcanic rocks within the basement that have been identified at five ODP sites (915A, 916A, 917A, 918D, and 990A) show red weathering, oxidized flow tops consistent with subaerial eruption. Analyses of paleosols and alteration minerals within the basalts are further evidence that they formed subaerially [*Holmes*, 1998]. The landwardmost part was erupted onto continental crust as indicated by the velocity structure and demonstrated by Site 917 where basalts are underlain by continental sediments. The acoustic bedding that defines the volcanic flow units is truncated, indicating erosion and the possibility that these basalts may have been emplaced in an elevated setting. Farther seaward, beyond the COB, preservation of top lap of the dipping reflectors shows that little or no erosion took place prior to subsidence and sedimentation of the igneous basement from km 165 onward. Dipping reflectors are seen as deep as 2 s twt below the basement. The wide-angle velocity model shows that the extrusive layer is ~4 km thick at its thickest point. The oldest basalts associated with this complex have a maximum age of 56 Ma [*Tegner and Duncan*, 1999], and the dipping reflectors end just within magnetic chron C24n at ~53 Ma. Thus the entire ~100 km sequence was erupted in only 3 Ma. These dates and distances correspond to an opening half rate of 3.3 cm/yr for this side of the North Atlantic. An interpretation of the magnetic crypto-chrons within C24r led *Larsen and Saunders* [1998] to suggest that spreading half rates during initial accretion were as high as 4.5 cm/yr around kms 200–220 and decreased eastward. An average rate of ~3.3 cm/yr is consistent with their interpretation.

[27] The seaward dipping reflector sequence terminates at a marked change in the morphology of the top of igneous crust. From km 272 to km 315, the basement shows a rough, hummocky surface below which nothing is imaged by the reflection data (Figure 12b). Following *Planke et al.* [2000], we interpret this to mark a change from subaerial eruptions to submarine eruptions. The morphology change is coincident with the disappearance of the high-velocity lower crust. In addition, this section of crust was accreted over 2.2 My, yielding a half rate of 1.95 cm/yr, significantly slower than the earlier spreading rate.

[28] The rough basement morphology ends at ~km 315 and a smooth continuous reflector caps the basement for the next 50 km of section before a large volcanic pile is seen to disrupt the basement at km 370–380 (Figure 12c). Beneath the smooth top of basement are seaward dipping reflectors reminiscent of those associated with the subaerially erupted basalts. Their curvature and dip are much lower, however, and the overall reflectivity is restricted to a much thinner zone. For reasons discussed below, these are interpreted as deep marine basaltic sheet flows [see *Planke et al.*, 2000]. Magnetic anomalies show that the half spreading rate continued to slow and is on average ~1.7 cm/yr by this point. It is very unlikely that this second set of reflectors represents a return to subaerial volcanism, because the crust continues to thin over this interval. A change back to subaerial eruption would indicate a resumption of much more robust volcanism and higher productivity rates that would be expected to produce thicker crust.

5. Discussion

[29] The data presented in this paper show the development of a volcanic rifted margin from >30 km thick Precambrian crust to close to average thickness oceanic crust [*White et al.*, 1992]. When combined with age constraints provided by well defined magnetic anomaly patterns and ^{40}Ar-^{39}Ar dating of basalts from drill cores, the data place quantitative constraints on the magmatic productivity through time of the margin and give insights into the nature and dynamics of the underlying mantle during the formation of the margin. In this section, we discuss two key ideas that the data elucidate about the early opening history of the North Atlantic. First, the data map the early subsidence history of the nascent spreading center. Second, comparison to the conjugate Hatton Bank and shows that the early opening history was highly asymmetric, with the bulk of new crust apparently accreted to the Greenland margin.

5.1. Basement Morphology and Spreading Center Subsidence

[30] Extrusive basaltic flows show variable morphologies, and thus distinct reflection seismic properties, depending on emplacement environment [*Gregg and Fornari*, 1998; *Planke et al.*, 2000]. The division of the reflection data into different zones based on the basement morphology thus gives insight into the evolution of the spreading system responsible for the formation of this volcanic margin. The most important factors are water depth, magma supply rates, and the configuration of local basins into which the basalts erupt [*Planke et al.*, 2000]. Subaerial extrusions with robust magmatic supplies form large continuous sheet flows and are responsible for producing seaward dipping reflector sequences. Shallow water extrusions are commonly explo-

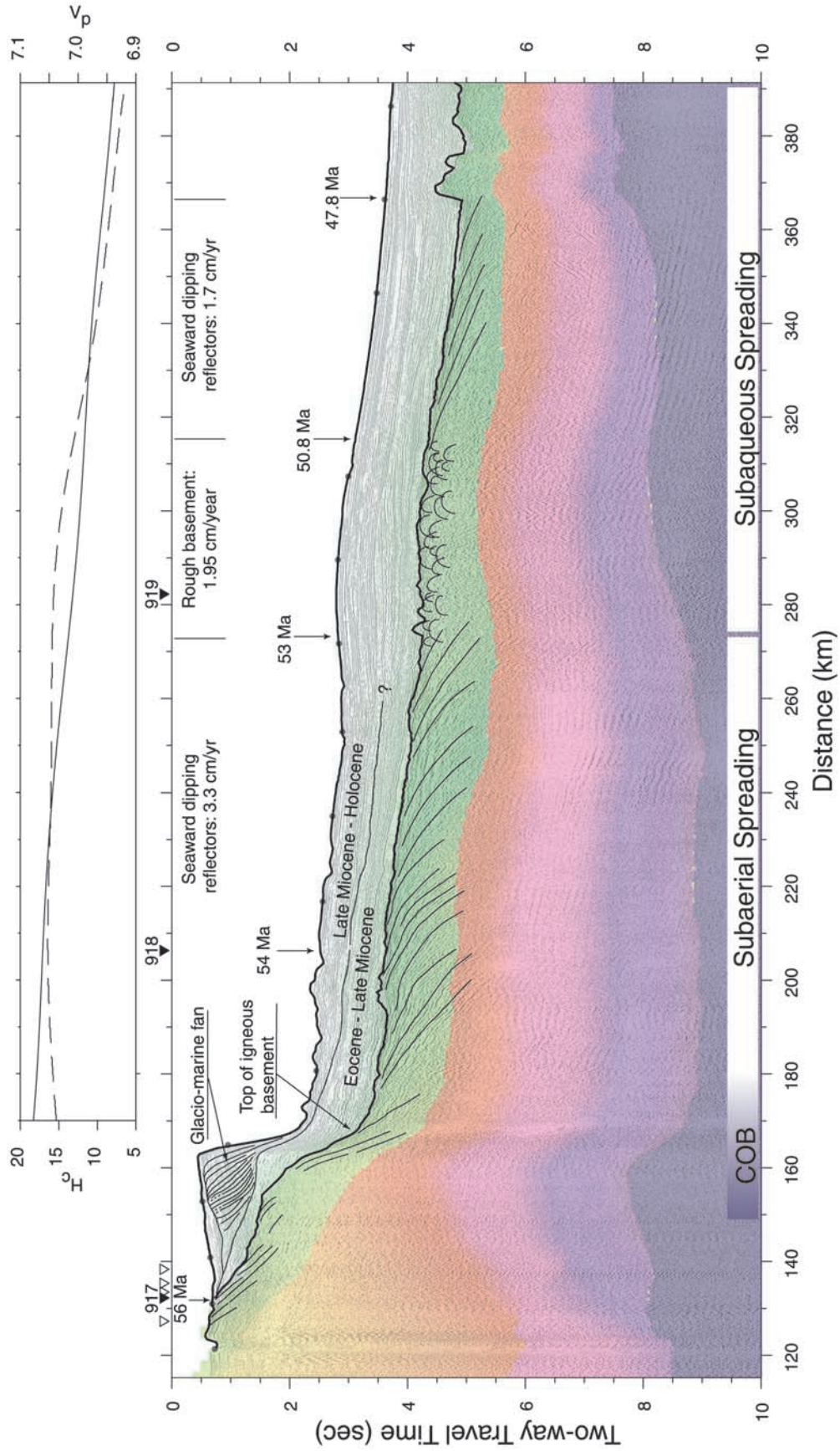

Figure 11. Interpreted MCS section. The color scale is the velocity model derived from the wide-angle data converted to two-way travel time. Same color scale as Figure 6. Major features are labeled and the gray dots along the seafloor are OBH/S stations.

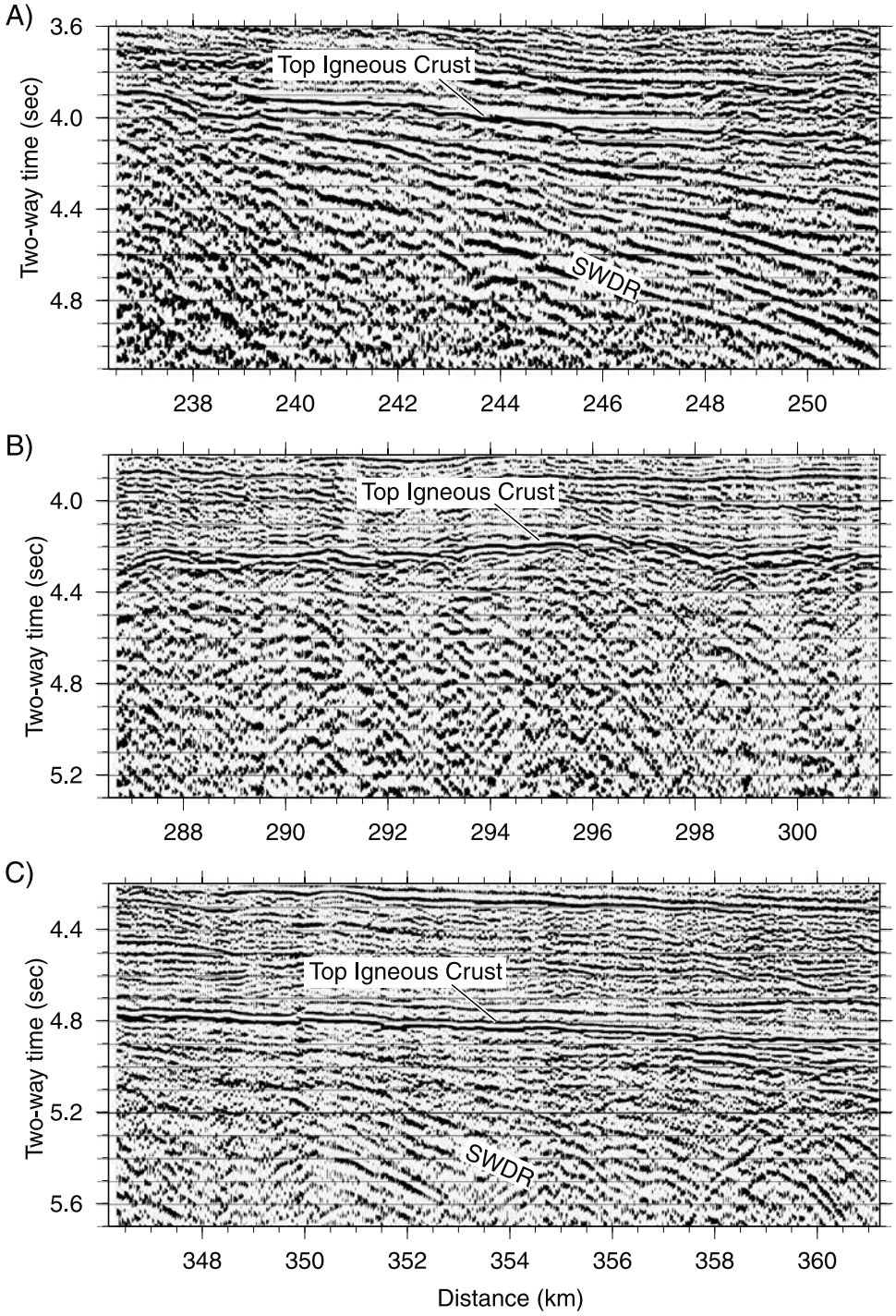

Figure 12. Details of seismic reflection data showing the different morphological zones discussed in the text. (a) Subaerially extruded basalts from the main seaward dipping reflector sequence. (b) Shallow marine extrusions. (c) Deep marine extrusions that generate long linear sheet flows and seaward dipping reflectors.

sive due to magma degassing. This results in hyaloclastite flows that are chaotic and laterally variable, forming a highly diffractive, rough surface on seismic images. Basalts erupted in deep water, however, may not degas, preventing the formation of hyaloclastites. In these conditions, large sheet flows can form if the magmatic supply is sufficient to overflow seafloor topography [*Gregg and Fornari*, 1998]. Such an environment is thought to be responsible for the creation of seaward dipping reflectors in oceanic crust [e.g., *Planke et al.*, 2000].

[31] The reflection data shown here record a history of changing eruptive environment with the key control being the elevation of the active spreading system relative to sea level. Margin subsidence is typically envisioned as resulting from crustal thinning and postrift thermal cooling of either thinned continental lithosphere [e.g., *McKenzie*, 1978] or

new oceanic lithosphere [e.g., *Parsons and Sclater*, 1977]. Dynamic mantle support can lead to significant subsidence anomalies and has been invoked to explain discrepancies between predicted and observed subsidence rates along the North Atlantic margins [*Clift et al.*, 1995]. By providing additional information on paleoelevation and vertical motion, the basement morphology can yield important constraints on margin subsidence. More importantly, because the basement morphology records the vertical motions of the seafloor spreading system itself, it provides a more direct link to mantle dynamic processes that operate during volcanic margin formation.

[32] The paleoelevation and subsidence of the most landward and oldest part of the basalt complex is constrained by ODP Sites 915, 916, 917 and 990 (Figures 2 and 11). A thin layer of volcaniclastic to conglomeratic sediments on top of the altered basalts is overlain by shallow water sediments of Middle to Late Eocene age. The subsidence rates indicated for the Middle Eocene is low, on the order of only 40 m/m.y. [*Wei*, 1998]. Given the significant hiatus between the igneous basement (~55 Ma) and the oldest datable marine sediments, it is unlikely that the crust here subsided below sea level immediately after its formation. To obtain a minimum estimate of the likely paleoelevation, we extrapolate the 40 m/m.y. subsidence rate back in time. This would place the rift system from which the basalts erupted at ~600 m above sea level. Eruption in an elevated area is consistent with these units being eroded as indicated by the truncation of the top lap described earlier.

[33] ODP Site 918 within the central part of the main seaward dipping reflector zone provides the most important constraints on the paleoelevation and subsidence of the igneous crust, which is 17.1 km thick here (Figure 11). A decreasing frequency of lava eruption with time is indicated by increasing weathering of individual flow units up section, with the last few flow units almost completely altered by weathering. *Holmes* [1998] suggests that this weathering took place in low lying rather than upland areas based on goethite/hematite ratios. In strong support of this, shallow water sediments of the same magnetic polarity are found immediately on top of these deeply weathered flows [*Ali and Vandamme*, 1998] and independent biostratigraphic data confirm that they are stratigraphically continuous with the lava flows [*Wei*, 1998]. In addition, the well preserved top lap of the seaward dipping reflectors shows that little to no erosion of the basalts occurred throughout this part of the section, indicating that the bulk of the igneous crust from at least Site 918 and seaward erupted in lowland areas.

[34] The major change in reflectivity and basement morphology that indicates a transition from subaerial to subaqueous extrusion occurs 60 km seaward of Site 918 and by this point new crust created was 13.5 km thick. DSDP Sites 552–554 off the Edoras Bank (Figure 2) sampled basalts in a similar setting and the recovery of hyaloclastites supports the idea of a transition into shallow water volcanism [*Roberts et al.*, 1984]. Along the Greenland margin, the timing of the drowning of the spreading ridge is 53 Ma and is tightly controlled by well-defined seafloor magnetic isochrons C24n2-n3. Thus, during the first 2 m.y. of margin formation, subaerial volcanism may have taken place at moderate elevations, but for at least the last 1 m.y. from Site 918 seaward, accretion of new crust must have been at or close to sea level. The apparent constancy of the paleoelevation, despite the fact that a decrease in volcanic productivity led to a reduction in crustal thickness from ~17 km to ~13.5 km over this interval, implies that the elevation of the spreading center must have been maintained by some dynamic support in the mantle that was removed as the margin evolved. Assuming local isostacy, the crustal thickness change should have resulted in subsidence on the order of 0.5 km and a much earlier submergence of the ridge system.

[35] Recent numerical models of lithospheric extension show that excess volcanism during breakup is likely the result of a combination of active upwelling and temperature anomalies [*Boutilier and Keen*, 1999; *Keen and Boutilier*, 2000; *Nielsen and Hopper*, 2002]. In these models, small-scale convection cells develop at the edge of a rifting continent and can enhance melt productivity. *Nielsen and Hopper* [2002] suggest that for this mechanism to produce the observed time and spatial scales of igneous productivity along SE Greenland, a thermal anomaly is required. This may provide a source of dynamic support to the rift system that can maintain it at sea level despite reduced productivity. Exhaustion of the thin sheet of material would result in subsidence as the source of support is removed.

[36] Along East Greenland, Figure 10 shows that the first igneous crust produced requires at least some component of active upwelling. Initially, the trend follows an isotherm, implying that thinner crust is a result of a reduction in active upwelling. What is less clear given the ambiguities and uncertainties regarding the method, is whether or not there is also evidence for a thermal anomaly. If residual crack porosity and alteration is indeed a problem for crust thinner than 15 km [*Korenaga et al.*, 2002], then it seems apparent that little can be learned from the H_c-V_p systematics on volcanic margins such as this. However, if for the sake of argument we accept the interpretation suggested earlier that a modest thermal anomaly may be indicated and that the reduction of seismic velocity is related to exhaustion of a thin sheet of plume material emplaced in a thin spot, then the inflection point in the H_c-V_p diagram correlates with the independent evidence just described for a major change in the emplacement environment of the extrusive layer. While this may be just a coincidence, the possibility that the morphology change can be related to changes in the upwelling dynamics of the mantle is an intriguing suggestion worthy of further investigation.

[37] The subsequent accretion of thinner crust from 13.5 km to 9 km should be accompanied by continued subsidence of the spreading system until a steady state ridge system is established. This is fully consistent with our interpretation that the second major change in reflectivity and morphology to a smooth basement top at 50.8 Ma (km 315) is a result of extrusion in deep water with high magma supply rates to feed large submarine sheet flows. To fully quantify the subsidence, constraints on the pressure and water depth required to prevent degassing of the magma are needed. *Gregg and Fornari* [1998] claim that volatiles remain dissolved in basaltic magma at pressures greater than 15 MPa, corresponding to a water depth of 1.5 km. Subsidence from sea level at 53 Ma to 1.5 km at 50.8 Ma would yield extreme rates on the order of 700 m/m.y. For comparison, this is nearly double what simple half-space

cooling of oceanic lithosphere can produce, but is similar to what has been reported for initial subsidence rates on other volcanic margins such as the U.S. East Coast [e.g., *Lizarralde and Holbrook*, 1997]. We note, however, that the present water depth of the Reykjanes Ridge along a flow line that connects to the SIGMA III profile is ~900 m. Crustal thickness estimates along the Reykjanes Ridge (8.5–10 km [*Smallwood et al.*, 1995]) are comparable to the thicknesses observed at the end of the SIGMA profile (9–11 km). It seems likely that the outer set of seaward dipping reflectors erupted from a spreading system at a similar water depth. This would yield a considerably smaller estimate of the subsidence rate, but still larger than postrift subsidence rates farther west over thick crust (site 918). In the absence of better data constraining the pressures required to enable long submarine flows, we can only conclude that continued subsidence of the spreading axis and a rapid deepening relative to the margin is indicated by our data but the magnitude and rates cannot be determined with confidence.

5.2. Asymmetric Crustal Accretion During Early Opening

[38] Volcanic conjugate margin asymmetry has been suggested previously [*Eldholm and Grüe*, 1994] and has important implications for quantifying magmatic productivity and volumes associated with early opening of the North Atlantic. To investigate this further, we compared the SIGMA III data to earlier seismic refraction along the Hatton Bank margin. Deep seismic data from the Hatton Bank is much older and is summarized in three key papers: *Spence et al.* [1989], *Fowler et al.* [1989], and *Morgan et al.* [1989]. The main profile, NI8, is ~75 km south of the conjugate position from SIGMA III predicted by reconstructions using poles of rotation from *Srivastava and Tapscott* [1986]. Flow lines from the ends of NI8 and SIGMA III to their conjugate positions are shown in Figure 1 and there is no apparent segmentation at this part of the early spreading axis. The NI8 transect consists of a reflection profile as well as several ESP's and an OBS refraction line coincident with the reflection line. Some caution should be exercised in comparing the SIGMA data to the Hatton Bank data because ESP's sample along strike, and the OBS profile consisted of widely spaced instruments with an explosive source. While general comparisons are possible, a detailed comparison of the velocity structure is not. In addition, detailed constraints on timing are less certain. Seafloor spreading anomalies are much less distinct and can only be convincingly identified back to anomaly C20. Identification of anomalies older than this is ambiguous at best, but the NI8 profile ends in a negative anomaly that likely corresponds to C21, placing anomaly C22 just seaward of ESP H (Figure 1b). Sediments interbedded with lava flows that are associated with the seaward dipping reflector sequence have been dated to 56 Ma [*Roberts et al.*, 1984], indicating that main flood basalt volcanism along the margin was contemporaneous with that on the Greenland side.

[39] Figure 13 shows the Hatton Bank data merged with the SIGMA data at approximately C22 time. The most striking observation shown in the comparison is the extreme asymmetry that is apparent by a quick visual inspection. The Greenland margin appears to have nearly double the volume of igneous crust as the Hatton Bank. Along the coast of east Greenland between SIGMA I and II, major plutons and dikes that range in age from 35 to 50 Ma have been extensively documented [*Bernstein et al.*, 1998]. A 52 Ma sill recovered within marine sediments at ODP site 918 could be evidence for similar volcanism along the SIGMA III profile. This late stage volcanism has been interpreted to represent the passage of the Iceland plume beneath the East coast of Greenland and there is the possibility that this could have added significant extra crust to the margin. However, we find it difficult to support the idea that this could explain a doubling in the crustal volume after initial accretion. First, significant off axis volcanism should disturb the magnetic spreading anomalies, which are exceptionally clear along East Greenland and can be interpreted down to the crypto-chron scale [*Larsen and Saunders*, 1998]. Second, the SIGMA III transect is in the so-called distal zone, well south of the region clearly affected by active upwelling associated with plume [*Holbrook et al.*, 2001]. Third, such significant magmatic events would disrupt the crustal structure and the smooth variation in crustal thickness and seismic velocity would not be seen. Last, it seems likely this magmatism would have an extrusive counterpart that should be imaged on the reflection sections as mounds and plateaus lying unconformably above the dipping reflector basement. The two features that disrupt the basement at km 370–380 may well represent such off axis volcanism. However, there is no evidence for similar features within the 56 Ma to 50 Ma crust (Figures 3 and 11).

[40] A second possible explanation is that a series of east directed ridge jumps transferred material to the Greenland margin. *Müller et al.* [1998] argue that most of the asymmetry in spreading anomalies they find in their global reconstructions can be related to ridge jumping toward a plume. We discount this as a possibility along East Greenland for several reasons. First, ridge jumping should be easily observable in the seismic reflection data over the seaward dipping reflectors. In the *Palmason* [1980] model, the extrusive flows dip toward the spreading axis. A reversal of the basalt stratigraphy dip would therefore be predicted by a ridge jump, and has in fact been observed on data along the Greenland-Iceland ridge where such jumping is common [*Larsen and Jakobsdottir*, 1988]. No such reversal is seen in the data. On both margins, the basalt flows dip consistently seaward, indicating that ridge jumping is unlikely. Second, most reconstructions place the Iceland hot spot beneath Greenland at the time of breakup [e.g., *Lawver and Müller*, 1994]. Thus plume-directed jumps would result in west rather than east directed ridge jumping, which is the opposite of our observation. Last, ridge jumps tend to disturb magnetic seafloor anomalies leaving complicated patterns behind. It seems unlikely that crypto-chron scale magnetic anomalies could be preserved if ridge jumping were an important process during the early formation of the margin [*Larsen and Saunders*, 1998].

[41] Thus the asymmetry in productivity appears to be a process related to original crustal accretion and the consistency of key features supports this idea. The maximum igneous crustal thickness accreted to each margin is roughly the same: 18.3 km on the Greenland and 18.5 km on the Hatton Bank side [*Morgan et al.*, 1989]. On both sides,

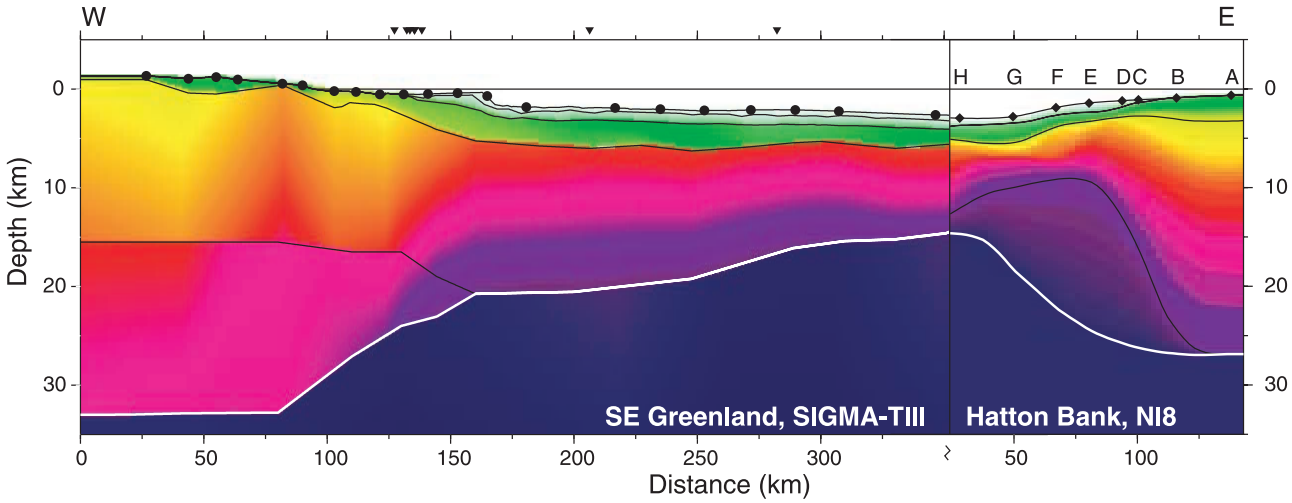

Figure 13. North Atlantic crustal profile at anomaly 22 time. Hatton Bank profile was digitized and gridded from *Fowler et al.* [1989]. Color scale is the same as Figure 6. Lower white line is Moho. Triangles along the top are ODP drilling sites. Dots on the Greenland side are the OBH/S and REFTEX stations.

evidence for an unusually high-velocity lower crust (>7.3 km/s) is restricted, and terminates seaward roughly where the main seaward dipping reflectors terminate. A progressive thinning of the new crust created is indicated from the time of breakup and the match in crustal structure at the splice point is remarkable given the uncertainties in anomaly identification and a 75 km offset in conjugate position. These similarities combined with the fact that we consider it difficult to imagine that a spreading system could produce crust of unequal thickness on each side, leads us to conclude that the asymmetry is primarily a difference in the horizontal length scale and thus is an accretional process. On Hatton Bank, the change from 18 km thick crust to 10 km thick crust occurs after only 50–60 km of spreading. However, on the SE Greenland margin, this reduction in igneous productivity occurs after 120 km of spreading. This observation is consistent with recent independent reconstructions of the North Atlantic by *Müller et al.* [1998], who show that ~65% of the initial crustal accretion along this part of the margin was accreted to the Greenland margin.

[42] A key issue to address is whether or not this asymmetry also reflects an asymmetry in total extension taken up by each side of the rift. In other words, did Greenland effectively spread at double the rate as Europe? It is possible that the magmatic extension that is apparently missing on Hatton Bank is taken up farther east on the Rockall Plateau and Trough. *Joppen and White* [1990] show that this latter region was clearly affected by Tertiary volcanism, but reliable estimates of the volumes and ages are unfortunately lacking. However, the missing volume is substantial, nearly 825 km^3/km along the rift. It seems unlikely that such enormous quantities of magmatic extension would be missed by the earlier seismic surveys carried out in the region [e.g., *England and Hobbs*, 1997; *Hauser et al.*, 1995; *Joppen and White*, 1990]. Thus we conclude that two thirds of the total extension was accommodated on the Greenland margin. Effectively, two out of every three dikes must have accreted to the western side of the rift system. Whether or not this asymmetry is plate scale or occurred only along this part of the Greenland margin requires further study, but preliminary evidence suggests that accretion was more symmetric farther south where SIGMA IV and the Edoras Bank profiles are located [*Holbrook et al.*, 2001].

[43] Asymmetric accretion at divergent plate boundaries has been described previously and has been attributed to migration of the ridge axis over the asthenosphere which skews the thermal field and/or leads to differences in shear tractions at the base of the two plates on either side of the axis [*Barker and Hill*, 1980; *Stein et al.*, 1977; *Hayes*, 1976]. In the thermal model, faster accretion is predicted on the cooler plate [*Hayes*, 1976; *Barker and Hill*, 1980]. This may be consistent with the Greenland margin being bounded by thick Archean lithosphere, whereas the Hatton Bank is bounded by younger and presumably warmer lithosphere beneath the Rockall Plateau. More recent mid-ocean ridge studies that consider asymmetry generally are intended to explain difference in topography, gravity, and seismic velocity on either side of a ridge [e.g., *Eberle and Forsyth*, 1998; *Toomey et al.*, 2002], but the implications for accretional processes have not been considered in these latter models. It seems clear, however, that the observation in Figure 13 is a first-order phenomenon and a full understanding of volcanic margin formation requires knowledge of magma emplacement processes and the crustal stress field in addition to the underlying mantle dynamics.

6. Conclusions

[44] Seismic data from the SE Greenland margin provide detailed information on margin structure from Archean continental crust to near-to-average oceanic crust. Key results are that the continent-ocean boundary is an abrupt, <50 km wide transition, with a relatively minor amount of continental thinning indicated prior to breakup. The maximum thickness of igneous crust accreted to the continent is 18.3 km and is reduced uniformly to ~9 km thick over a distance of 160 km. Average V_p in the accreted igneous crust is constant for the first 3 m.y. of evolution and then decreases uniformly from 7.05 km/s to 6.9 km/s. Although we cannot rule out the possibility that residual crack

porosity is responsible for this decrease in average velocity, this could be evidence that the mantle potential temperature stayed constant for a short period of time, and then dropped. The uniform decrease in crustal thickness over the time interval that the mantle potential temperature was constant may indicate that a small component of active upwelling enhanced initial melt production.

[45] Distinct changes in morphology of the extrusive basalt layer in the crust are interpreted as evidence for submergence of the rift system below sea level at 53 Ma. An additional change in basement morphology and a second but poorly developed seaward dipping reflector sequence is evidence for continued subsidence from shallow water to deeper water, likely between 900 and 1500 m. Subsidence of the active spreading axis is evidence for dynamic support to the margin during the early opening history that was gradually removed as the system evolved to steady state oceanic accretion.

[46] These interpretations of the seismic velocity data and seismic reflection data are both consistent with recent suggestions that plume material was emplaced along thin spots prior to North Atlantic opening. Exhaustion of the thin warm sheet led to a loss of dynamic support and subsidence of the active ridge axis. At the same time, cooler mantle began upwelling beneath the spreading axis and the average depth of melting decreased, as shown by the reduction in average seismic velocity of accreted igneous crust.

[47] Perhaps more significantly, comparison to the conjugate Hatton Bank data demonstrates that volcanic margin formation can be extremely asymmetric. During the first 5–6 m.y. of spreading, double the volume of crust apparently accreted to the Greenland margin compared to the Hatton Bank margin. Ridge jumps and late stage volcanism cannot explain this observation. Effectively, the ridge system must have been migrating eastward. This appears to be a regional rather than plate scale phenomenon, but more detailed along strike comparisons are necessary. It seems likely that accretional asymmetry requires a process that allows more dikes and extrusives to pile up on one side of the spreading system. The observation of large-scale asymmetry points to the need for better planned conjugate margin studies to fully unravel the history of breakup and the onset of seafloor spreading even in high magmatic productivity environments. Asymmetry is a first-order observation that dynamic models of volcanic margin formation and mid-ocean ridge spreading should seek to explain.

[48] **Acknowledgments.** We thank the captain and crew of the R/V *Maurice Ewing* for a successful cruise despite the difficulties of working in the North Atlantic. We also thank Rob Handy, Jim Dolan, Dave Dubois, Bob Busby, Paul Henkart, Thomas Nielsen, and Anders Bruun for their work at sea and Stefan Bernstein for his work on land deploying the REFTEK instruments. Barrie Taylor at Landmark Graphics Corp. is gratefully acknowledged for recovering data from bad tapes. Bob Detrick helped get the project off the ground and provided comments on an early version of the manuscript. Reviews from Tim Minshull and Tim Reston helped improve the manuscript. MCS data processing was done using the NSF supported software SIOSEIS and the commercial software ProMAX™. SIGMA was funded by the Danish National Research Foundation (Danmarks Grundforskningsfond) and U.S. NSF grant OCE-9416631.

References

Ali, J. R., and D. Vandamme, Eocene-Miocene magnetostratigraphy of the southeast Greenland margin and western Irminger Basin, *Proc. Ocean Drill. Program Sci. Results*, *152*, 253–257, 1998.

Allen, R. M., et al., Plume-driven plumbing and crustal formation in Iceland, *J. Geophys. Res.*, *107*(B8), 2163, doi:10.1029/2001JB000584, 2002.

Barker, P. F., and I. A. Hill, Asymmetric spreading in back-arc basins, *Nature*, *285*, 652–654, 1980.

Barton, A. J., and R. S. White, Crustal structure of the Edoras Bank margin and mantle thermal anomalies beneath the North Atlantic, *J. Geophys. Res.*, *102*, 3109–3129, 1997.

Bernstein, S., P. B. Kelemen, C. Tegner, M. D. Kurz, J. Blusztajn, and C. K. Brooks, Post-breakup basaltic magmatism along the East Greenland Tertiary rifted margin, *Earth Planet. Sci. Lett.*, *160*, 845–862, 1998.

Boutilier, R. R., and C. E. Keen, Small-scale convection and divergent plate boundaries, *J. Geophys. Res.*, *104*, 7389–7403, 1999.

Chalmers, J. A., and K. H. Laursen, Labrador Sea: The extent of continental and oceanic crust and the timing of the onset of seafloor spreading, *Mar. Pet. Geol.*, *12*, 205–217, 1995.

Chian, D., and K. E. Louden, The structure of Archean-Ketilidian crust along the continental shelf of southwestern Greenland from a seismic refraction profile, *Can. J. Earth Sci.*, *29*, 301–313, 1992.

Clift, P. D., J. Turner, and Ocean Drilling Program Leg 152 Scientific Party, Dynamic support by the Icelandic plume and vertical tectonics of the northeast Atlantic continental margins, *J. Geophys. Res.*, *100*, 24,473–24,486, 1995.

Dahl-Jensen, T., T. B. Larsen, I. Woelbern, T. Bach, W. Hanka, R. Kind, S. Gregersen, K. Mosegaard, P. Voss, and O. Gudmundsson, Depth to Moho in Greenland: Receiver function analysis suggests two Proterozoic Blocks in Greenland, *Earth Planet. Sci. Lett.*, doi:10.106/S0012-821X(02)01080-4, 379–393, 2003.

Eberle, M. A., and D. W. Forsyth, Evidence from the asymmetry of fast-spreading ridges that the axial topographic high is due to extensional stresses, *Nature*, *394*, 360–363, 1998.

Eldholm, O., and K. Grüe, North Atlantic volcanic margins: Dimensions and production rates, *J. Geophys. Res.*, *99*, 2955–2968, 1994.

Eldholm, O., et al., *Proceedings of the Ocean Drilling Program, Scientific Results*, vol. 104, Ocean Drill. Program, College Station, Tex., 1989.

England, R. W., and R. W. Hobbs, The structure of the Rockall Trough imaged by deep seismic reflection profiling, *J. Geol. Soc. London*, *154*, 497–502, 1997.

Fowler, S. R., R. S. White, G. D. Spence, and G. K. Westbrook, The Hatton Bank continental margin—II. Deep structure for two-ship expanding spread seismic profiles, *Geophys. J. Int.*, *96*, 295–309, 1989.

Funck, T., and K. E. Louden, Wide-angle seismic imaging of pristine Archean crust in the Nain Province, Labrador, *Can. J. Earth Sci.*, *35*, 672–685, 1998.

Gregg, T. K. P., and D. J. Fornari, Long submarine lava flows: Observations and results from numerical modeling, *J. Geophys. Res.*, *103*, 27,517–27,531, 1998.

Griffiths, R. W., and I. H. Campbell, Stirring and structure in mantle starting plumes, *Earth Planet. Sci. Lett.*, *99*, 66–78, 1990.

Hauser, F., B. M. O'Reilly, A. W. B. Jacob, P. M. Shannon, J. Makris, and U. Vogt, The crustal structure of the Rockall Trough: Differential stretching without underplating, *J. Geophys. Res.*, *100*, 4097–4116, 1995.

Hayes, D. E., Nature and implications of asymmetric sea-floor spreading—"Different rates for different plates", *Geol. Soc. Am. Bull.*, *87*, 994–1002, 1976.

Hill, R. I., Starting plumes and continental break-up, *Earth Planet. Sci. Lett.*, *104*, 398–416, 1991.

Hinz, K., J. C. Mutter, and C. M. Zehnder, Symmetric conjugation of continent-ocean boundary structures along the Norwegian and East Greenland margins, *Mar. Pet. Geol.*, *3*, 166–187, 1987.

Holbrook, W. S., H. C. Larsen, J. Korenaga, T. Dahl-Jensen, I. D. Reid, P. B. Kelemen, J. R. Hopper, G. M. Kent, D. Lizarralde, S. Bernstein, and R. S. Detrick, Mantle thermal structure and active upwelling during continental breakup in the North Atlantic, *Earth Planet. Sci. Lett.*, *190*, 251–266, 2001.

Holmes, M. A., Alteration of uppermost lavas and volcaniclastics recovered during Leg 152 to the East Greenland margin, *Proc. Ocean Drill. Program, Sci. Results*, *152*, 115–128, 1998.

Joppen, M., and R. S. White, The structure and subsidence of Rockall Trough from two-ship seismic experiments, *J. Geophys. Res.*, *95*, 19,821–19,837, 1990.

Keen, C. E., and R. R. Boutilier, Interaction of rifting and hot horizontal plume sheets at volcanic margins, *J. Geophys. Res.*, *105*, 13,375–13,387, 2000.

Kelemen, P. B., and W. S. Holbrook, Origin of thick, high-velocity igneous crust along the U.S. East Coast Margin, *J. Geophys. Res.*, *100*, 10,077–10,094, 1995.

Korenaga, J., and P. B. Kelemen, Major element heterogeneity in the mantle source of the North Atlantic igneous province, *Earth Planet. Sci. Lett.*, *184*, 251–268, 2000.

Korenaga, J., W. S. Holbrook, G. M. Kent, P. B. Kelemen, R. S. Detrick, H. C. Larsen, J. R. Hopper, and T. Dahl-Jensen, Crustal structure of the southeast Greenland margin from joint refraction and reflection seismic tomography, *J. Geophys. Res.*, *105*, 21,591–21,614, 2000.

Korenaga, J., P. B. Kelemen, and W. S. Holbrook, Methods of resolving the origin of large igneous provinces from crustal seismology, *J. Geophys. Res.*, *107*, 2178, doi:10.1029/2001JB001030, 2002.

Larsen, H. C., and S. Jakobsdottir, Distribution, crustal properties and significance of seawards-dipping sub-basement reflectors off E Greenland, in *Early Tertiary Volcanism and the Opening of the NE Atlantic*, edited by A. C. Morton and L. M. Parson, *Geol. Soc. Spec. Publ.*, *39*, 95–114, 1988.

Larsen, H. C., and A. D. Saunders, Tectonism and volcanism at the southeast Greenland rifted margin: A record of plume impact and later continental rupture, *Proc. Ocean Drill. Program Sci. Results*, *152*, 503–534, 1998.

Larsen, H. C., T. Dahl-Jensen, and J. R. Hopper, Crustal structure along the Leg 152 drilling transect, *Proc. Ocean Drill. Program, Sci. Results*, *152*, 463–475, 1998.

Larsen, H. C., et al., *Proceedings of the Ocean Drilling Program, Scientific Results*, vol. 163, Ocean Drill. Program, College Station, Tex., 1999.

Larsen, L. M., R. Waagstein, A. K. Pedersen, and M. Storey, Trans-Atlantic correlation of the Paleogene volcanic successions in the Faeroe Islands and East Greenland, *J. Geol. Soc. London*, *156*, 1081–1095, 1999.

Lawver, L. A., and R. D. Müller, Iceland hot-spot track, *Geology*, *22*, 311–314, 1994.

Lizarralde, D., and W. S. Holbrook, U.S. mid-Atlantic margin structure and early thermal evolution, *J. Geophys. Res.*, *102*, 2855–2875, 1997.

Macnab, R., J. Verhoef, and S. Srivastava, A new database of magnetic observations from the Arctic and North Atlantic oceans, in *Current Research, Part D, Eastern Canada and National and General Programs*, pp. 173–178, Geol. Surv. of Can., Ottawa, 1992.

McKenzie, D. P., Some remarks on the development of sedimentary basin, *Earth Planet. Sci. Lett.*, *40*, 25–32, 1978.

McKenzie, D. P., and M. J. Bickle, The volume and composition of melt generated by extension of the lithosphere, *J. Petrol.*, *29*, 625–679, 1988.

Morgan, J. V., P. J. Barton, and R. S. White, The Hatton Bank continental margin—III. Structure from wide-angle OBS and multichannel seismic refraction profiles, *Geophys. J. Int.*, *98*, 367–384, 1989.

Müller, R. D., W. R. Roest, and J.-Y. Royer, Asymmetric sea-floor spreading caused by ridge-plume interactions, *Nature*, *396*, 455–459, 1998.

Mutter, J. C., and C. Z. Mutter, Variations in thickness of layer 3 dominate oceanic crustal structure, *Earth. Planet. Sci. Lett.*, *117*, 295–317, 1993.

Mutter, J. C., and C. M. Zehnder, Deep crustal and magmatic processes: The inception of seafloor spreading in the Norwegian-Greenland Sea, in *Early Tertiary Volcanism and the Opening of the NE Atlantic*, edited by A. C. Morton and L. M. Parson, *Geol. Soc. Spec. Publ.*, *39*, 35–48, 1988.

Nielsen, T. K., and J. R. Hopper, Formation of volcanic rifted margins: Are temperature anomalies required?, *Geophys. Res. Lett.*, *29*(21), 2022, doi:10.1029/2002GL015681, 2002.

Nielsen, T. K., H. C. Larsen, and J. R. Hopper, Contrasting rifted margin styles south of Greenland: Implications for mantle plume dynamics, *Earth and Planet. Sci. Lett.*, *200*, doi:10.1016/S0012-821X(02)0,616-7, 270–285, 2002.

Palmason, G., A continuum model of crustal generation in Iceland: Kinematic aspects, *J. Geophys.*, *47*, 7–18, 1980.

Parsons, B., and J. G. Sclater, An analysis of the variation of the ocean floor bathymetry and heat flow with age, *J. Geophys. Res.*, *82*, 803–827, 1977.

Pearson, D. G., C. H. Emeleus, and S. P Kelley, Precise $^{40}Ar/^{39}Ar$ age for the initiation of Palaeogene volcanism in the Inner Hebrides and its regional significance, *J. Geol. Soc. London*, *153*, 815–818, 1996.

Planke, S., P. A. Symonds, E. Alvestad, and J. Skogseid, Seismic volcanostratigraphy of large-volume basaltic extrusive complexes on rifted margins, *J. Geophys. Res.*, *105*, 19,335–19,351, 2000.

Reid, I., Crustal structure across the Nain-Makkovik boundary on the continental shelf off Labrador from seismic refraction data, *Can. J. Earth. Sci.*, *33*, 460–471, 1996.

Roberts, D. G., et al., *Initial Reports of the Deep Sea Drilling Project*, vol. 81, U.S. Govt. Print. Off., Washington, D. C., 1984.

Rudnick, R. L., and D. M. Fountain, Nature and composition of the continental crust: A lower crustal perspective, *Rev. Geophys.*, *33*, 267–309, 1995.

Saunders, A. D., et al., *Proceedings of the Ocean Drilling Program, Scientific Results*, vol. 152, Ocean Drill. Program, College Station, Tex., 1998.

Sinton, C. W., and R. A. Duncan, ^{40}Ar-^{39}Ar ages of lavas from the southeast Greenland margin, ODP Leg 152, and the Rockall Plateau, DSDP Leg 81, *Proc. Ocean Drill. Program Sci. Results*, *152*, 387–402, 1998.

Skogseid, J., T. Pedersen, O. Eldholm, and B. T. Larsen, Tectonism and magmatism during NE Atlantic continental break-up: The Vøring Margin, in *Magmatism and the Causes of Continental Breakup*, edited by B. Storey, T. Albaster, and R. J. Pankhurst, *Geol. Soc. Spec. Publ.*, *68*, 305–320, 1992.

Smallwood, J. R., R. S. White, and T. A. Minshull, Sea-floor spreading in the presence of the Iceland plume: The structure of the Reykjanes Ridge at 61°40′N, *J. Geol. Soc. London*, *152*, 1023–1029, 1995.

Smallwood, J. R., R. K. Staples, K. R. Richardson, and R. S. White, Crust generated above the Iceland mantle plume: From continental rift to oceanic spreading center, *J. Geophys. Res.*, *104*, 22,885–22,902, 1999.

Spence, G. D., R. S. White, G. K. Westbrook, and S. R. Fowler, The Hatton Bank continental margin—I. Shallow structure from two-ship expanding spread seismic profiles, *Geophys. J. Int.*, *96*, 273–294, 1989.

Srivastava, S. P., and W. R. Roest, Extent of oceanic crust in the Labrador Sea, *Mar. Pet. Geol.*, *16*, 65–84, 1999.

Srivastava, S. P., and C. R. Tapscott, Plate kinematics of the North Atlantic, in *The Geology of North America*, vol. M, *The Western North Atlantic Region*, edited by P. R. Vogt and B. E. Tucholke, pp. 379–404, Geol. Soc. of Am., Boulder, Colo., 1986.

Stein, S., H. J. Melosh, and J. B. Minster, Ridge migration and asymmetric sea-floor spreading, *Earth. Planet. Sci. Lett.*, *36*, 51–62, 1977.

Storey, M., R. A. Duncan, A. K. Pedersen, L. M. Larsen, and H. C. Larsen, ^{40}Ar-^{39}Ar geochronology of the West Greenland Tertiary volcanic province, *Earth Planet. Sci. Lett.*, *160*, 569–586, 1998.

Talwani, M., et al., *Initial Reports of the Deep Sea Drilling Project*, vol. 38, U.S. Govt. Print. Off., Washington, D. C., 1976.

Tegner, C., and R. A. Duncan, ^{40}Ar-^{39}Ar chronology for the volcanic history of the southeast Greenland rifted margin, *Proc. Ocean Drill. Program Sci. Results*, *163*, 53–62, 1999.

Tegner, C., C. E. Lesher, L. M. Larsen, and W. S. Watt, Evidence from the rare-earth-element record of mantle melting for cooling of the Tertiary Iceland plume, *Nature*, *395*, 591–594, 1998.

Toomey, D. R., W. S. D. Wilcock, F. A. Conder, S. W. Forsyth, J. D. Blundy, E. M. Parmentier, and W. C. Hammond, Asymmetric mantle dynamics in the MELT region of the East Pacific Rise, *Earth Planet. Sci. Lett.*, *200*, doi:10.1016/S0012-821X(02)0,655-6, 287–295, 2002.

Verhoef, J., R. Macnab, and S. P. Srivastava, New magnetic anomaly maps of the Arctic and North Atlantic oceans, *Proc. Int. Geol. Congr.*, *29*, 974, 1992.

Wei, W., Calcareous nannofossils from the southeast Greenland margin: Biostratigraphy and paleoceanography, *Proc. Ocean Drill. Program, Sci. Results*, *152*, 147–160, 1998.

White, R. S., and D. McKenzie, Magmatism at rift zones: The generation of volcanic continental margins and flood basalts, *J. Geophys. Res.*, *94*, 7685–7729, 1989.

White, R. S., D. McKenzie, and R. K. O'Nions, Oceanic crustal thickness from seismic measurements and rare earth element inversions, *J. Geophys. Res.*, *97*, 19,683–19,715, 1992.

Yilmaz, O., *Seismic Data Processing*, Soc. of Explor. Geophys., Tulsa, Okla., 1987.

Zelt, C. A., and R. B. Smith, Seismic traveltime inversion for 2-D crustal velocity structure, *Geophys. J. Int.*, *108*, 16–34, 1992.

T. Dahl-Jensen, Geological Survey of Denmark and Greenland, Øster Voldgade 10, DK1350 Copenhagen K, Denmark. (tdj@geus.dk)

W. S. Holbrook, Department of Geology and Geophysics, University of Wyoming, Laramie, WY 82071, USA. (steveh@uwyo.edu)

J. R. Hopper and H. C. Larsen, Danish Lithosphere Center, Øster Voldgade 10, DK1350 Copenhagen K, Denmark. (jrh@dlc.ku.dk; hcl@dlc.ku.dk)

G. M. Kent, Scripps Institution of Oceanography, University of California, San Diego, La Jolla, CA 92093, USA. (gkent@ucsd.edu)

P. B. Kelemen, Department of Geology and Geophysics, Woods Hole Oceanographic Institution, Woods Hole, MA 02543, USA. (pkelemen@whoi.edu)

J. Korenaga, Department of Geology and Geophysics, Yale University, P.O. Box 208109, New Haven, CT 06520-8109, USA. (jun.korenaga@yale.edu)

D. Lizarralde, School of Earth and Atmospheric Sciences, Georgia Institute of Technology, 221 Bobby Dodd Way, Atlanta, GA 30332, USA. (danl@eas.gatech.edu)